Pten Loss Triggers Progressive Photoreceptor Degeneration in an mTORC1-Independent Manner

Joseph Hanna,[1–3] Yacine Touahri,[1,3,4] Alissa Pak,[1,2] Luke Ajay David,[1–3] Edwin van Oosten,[1,4] Rajiv Dixit,[1,4] Laura M. Vecchio,[1,2] Dhruv Nimesh Mehta,[1] Ren Minamisono,[1] Isabelle Aubert,[1,2] and Carol Schuurmans[1–4]

[1]Biological Sciences Platform, Sunnybrook Research Institute, Toronto, Ontario, Canada
[2]Department of Laboratory Medicine and Pathobiology, University of Toronto, Toronto, Ontario, Canada
[3]Department of Ophthalmology and Vision Sciences, University of Toronto, Toronto, Ontario, Canada
[4]Department of Biochemistry, University of Toronto, Toronto, Ontario, Canada

Correspondence: Carol Schuurmans, Sunnybrook Research Institute, 2075 Bayview Ave, Room A340, Toronto, Ontario M4N 3M5, Canada; cschuurm@sri.utoronto.ca.

JH and YT contributed equally to the work presented here and should therefore be regarded as co-first authors.

Received: June 19, 2024
Accepted: February 19, 2025
Published: March 21, 2025

Citation: Hanna J, Touahri Y, Pak A, et al. *Pten* loss triggers progressive photoreceptor degeneration in an mTORC1-independent manner. *Invest Ophthalmol Vis Sci.* 2025;66(3):45. https://doi.org/10.1167/iovs.66.3.45

Purpose. Silencing Phosphatase and tensin homolog (*Pten*) is a proposed therapeutic strategy for tissue regeneration to treat neurological disorders. However, *Pten* is pleiotropic, inhibiting several signaling and metabolic pathways, including mTORC1 and glycolysis, both pro-regenerative in certain contexts. This study aims to assess the long-term impact of inactivating *Pten* on photoreceptor survival in the retina and to identify downstream pathway(s).

Methods. We assessed retinal integrity in *Pten* conditional knock-outs (cKOs) that were retinal progenitor cell (RPC)-specific (*Pten* RPC-cKO), a congenital model, or rod-specific (*Pten* Rho-cKO). We examined early changes in photoreceptor gene expression and used immunostaining to assess photoreceptors, reactive astrocytes, microglia, angiogenesis, and subretinal deposit formation from postnatal day (P) 21 to 1 year of age. *Pten* RPC-cKO retinal explants were treated with rapamycin, an mTOR inhibitor, or 2-deoxy-D-glucose (2DG), a glycolysis inhibitor.

Results. In both *Pten*-cKO models, retinas display signs of early pathogenesis as photoreceptor-specific gene expression is downregulated at P0, before photoreceptor loss. *Pten* loss triggers progressive rod and cone degeneration beginning at P21 in *Pten* RPC-cKOs and at 6 months of age in *Pten* Rho-cKOs. Activated microglia and astrocytes, and increased angiogenesis, are observed in both *Pten*-cKO models, while subretinal amyloid-β deposits develop in *Pten* RPC-cKOs. Rapamycin accelerates photoreceptor degeneration in *Pten* RPC-cKOs, whereas 2DG has no effect.

Conclusions. Our findings suggest that *Pten* loss, either in RPCs as a congenital model, or solely in mature rod photoreceptors, leads to progressive retinal degeneration that is exacerbated by mTORC1 suppression, drawing into question the therapeutic value of *Pten*-mTORC1 manipulations.

Keywords: *Pten* phosphatase, retinal progenitor cells (RPCs), rod photoreceptors, degeneration, β-amyloid

The retina is a multicellular tissue comprised of three main neural cell layers; a ganglion cell layer (GCL), an inner nuclear layer (INL), and an outer nuclear layer (ONL). The ONL contains the nuclei of light-sensing rod and cone photoreceptors, which account for 75% of all retinal cells.[1,2] Rod photoreceptors are activated by low light to allow for night vision, whereas cone photoreceptors are responsible for high acuity and color vision in daylight.[3] Of the two photoreceptor types, rods are by far more numerous, representing 95% to 97% of all photoreceptors in human and rodent retinas, respectively.[1,2] Rod and cone photoreceptors are born in the embryonic and early postnatal period and must survive to function throughout life.[4] Given their central role in phototransduction, photoreceptor cell death results in profound vision loss, and is currently an untreatable pathology.

Triggers for photoreceptor degeneration include inherited retinal dystrophies (IRDs)[5] and non-hereditary factors, such as aging, injury, and systemic disorders (e.g. diabetic retinopathy).[6] IRDs are associated with gene mutations that either directly impact photoreceptor function and survival, or that compromise the health of the retinal pigment epithelium (RPE),[7] an essential epithelial layer that provides nutrient and phototransduction support to photoreceptors.[5] Retinitis pigmentosa (RP) is a heterogeneous group of IRDs estimated to affect 1:4000 individuals worldwide.[1,2] Mutations in over 190 genes cause RP,[3] including in *Rhodopsin* (*Rho*), a light-sensitive opsin involved in rod cell

phototransduction.[5] Regardless of the underlying genetic cause, rod photoreceptors are the first to degenerate in RP, leading to peripheral vision loss and night blindness. As the disease progresses, cone photoreceptors degenerate as a secondary consequence of rod loss.[8–11] Conversely, in age-related macular degeneration (AMD), a major non-hereditary cause of blindness,[12] the loss or dysfunction of RPE cells overlying the cone-dense macula means that cone degeneration predominates early, resulting in central vision loss. Therapeutic strategies that effectively prevent photoreceptor degeneration in IRDs and AMD or promote repair are lacking.

Photoreceptors are among the most metabolically active cells in the body. Glucose is supplied to photoreceptors from RPE cells via the choroidal circulation. Photoreceptors metabolize glucose to lactate through aerobic glycolysis.[13] This lactate is transported back to the RPE and to Müller glial cells, where it is converted to pyruvate to fuel their mitochondria for oxidative phosphorylation, forming a metabolic ecosystem.[14–16] However, whereas both rod and cone photoreceptors can use glycolysis, rod photoreceptors also depend to a large extent on oxidative phosphorylation.[13] In photoreceptors, these metabolic pathways produce energy (i.e. ATP) and biomass,[17] which drive the continual turnover of photoreceptor outer segments (OSs) throughout life.[18] A key regulator of metabolism is mechanistic target of rapamycin (mTOR), an intracellular kinase that complexes with Raptor (mTORC1) or Rictor (mTORC2) to control the expression of glucose transporters and glycolytic enzymes.[19] The mTOR signaling pathway is nutrient-sensitive and operates downstream of insulin signaling to maintain homeostatic levels of glycolysis.

Cones depend on rods for nutrient support, with nutrient deprivation due to rod cell death serving as a central trigger for cone degeneration, in addition to the loss of trophic support and the buildup of toxic byproducts associated with rod loss.[20–30] In mouse models of RP, cone survival is improved upon mTOR activation, which can be achieved by cone-specific deletions of *Pten* or Tsc1, negative regulators of mTOR,[31] by overexpressing ribosomal protein S6 kinase-beta-1 (S6K1), a downstream mTOR effector,[32] or by systemic injection of insulin.[30] Similarly, rod-specific deletion of *Tsc1* improves rod and cone survival in a mouse model of RP.[33] Conversely, a cone-specific *Rptor*-conditional knock-out (cKO), which reduces mTORC1 signaling, accelerates cone degeneration in RP mice, albeit not in wild-type controls.[31] The pro-survival effects of mTORC1 may be mediated by glycolysis, since the rod-specific deletion of *Sirt6*, an HDAC that represses glycolytic flux, enhances photoreceptor survival in RP mice.[34] Conversely, deleting the glycolytic enzymes *Pfk* in rods[34] or *Hk2* in cones[35] exacerbates rod and cone photoreceptor degeneration, respectively, in mouse models of RP.[34]

These data support a pro-survival effect of mTORC1 and downstream glycolysis in photoreceptors. Yet, activation of mTORC1 signaling does not always have beneficial effects. For instance, in wild-type mice, rod- and cone-specific *Tsc1*-cKOs develop AMD-like pathologies, including microglia accumulation, geographic atrophy (GA), and neovascular abnormalities, whereas cone-specific *Tsc1*-cKOs also form drusen-like deposits.[36] Furthermore, rapamycin, which is a pharmacological inhibitor of mTOR signaling, preserves photoreceptor health in certain contexts, including in a methyl methanesulfonate-induced RP-like paradigm.[37] Similarly, rapamycin reverses the detrimental effects of LPS-mediated inflammation on rod photoreceptor gene expression and OS formation.[38] Consistent with the need for precise levels of mTOR signaling, co-deleting *Rptor/Rictor* in wild-type mice, which reduces mTORC1 and mTORC2 signaling, alters cone function and structure without impacting survival.[31,39] Thus, mTOR signaling has pro-survival effects for photoreceptors only in certain cellular contexts, including in RP models, in which photoreceptors are metabolically challenged, whereas blocking mTORC1 is beneficial in other inflammatory contexts.

PTEN is a lipid and protein phosphatase that negatively regulates PI3K signaling and downstream signal transduction molecules, including mTOR.[40,41] Additionally, *PTEN* inhibits glycolysis by dephosphorylating and inactivating PGK1, a rate-limiting glycolytic enzyme.[42] Thus, both mTOR signaling and glycolytic gene expression are elevated in *Pten*-deleted cells.[43] *Pten* knock-down has been touted as a promising regenerative strategy to repair severed axons in the nervous system, including in the retina, in which ganglion cell axonal regeneration is enhanced.[44,45] Moreover, in cone-specific *Pten*-cKOs, cone survival is prolonged.[30,31] However, targeting *Pten* is not without consequences. *Pten* deletion leads to defects in dendrite arborization and myelination and neuronal hypertrophy in the murine brain, and is associated with autism spectrum disorder in humans.[46] In retinal progenitor cell (RPC)-specific *Pten*-cKO mice, defects in interneuron cell spacing, axonal and dendritic arborization and retinal circuitry are observed.[47–52] In addition, here, we investigated the long-term consequences of *Pten* deletion on photoreceptor health using two models: a *Pten* RPC-cKO in which *Pten* was deleted in RPCs and, hence, in all retinal progeny, including photoreceptors, as a model of a congenital disorder; and a rod-specific *Pten* Rho-cKO. By investigating these mice up to 1 year of age, we found that *Pten* deletion reduces photoreceptor survival and induces inflammatory responses, with more severe effects observed when *Pten* is deleted in RPCs. Furthermore, rapamycin-mediated blockade of mTORC1 signaling further exacerbates the *Pten* RPC-cKO photoreceptor degeneration phenotype, whereas glycolytic inhibition had no effect. Thus, *Pten* is required to maintain photoreceptor survival, with further degenerative effects suppressed by elevated mTORC1 signaling.

Methods

Animals

Animal procedures were approved by the Sunnybrook Research Institute Animal Care Committee (16–606) in agreement with the Guidelines of the Canadian Council of Animal Care (CCAC) and in accordance with the Association for Research in Vision and Ophthalmology (ARVO) statement of animal use in ophthalmic and vision science research. Animals were housed in a 12-hour light/dark cycle and were fed ad libitum. Transgenic animals were obtained from Jackson Laboratory. *Pten* RPC-cKOs were generated using a *Pten*^{fl} allele (B6.129S4-*Pten*^{tm1Hwu}/J. Strain #: 006440, RRID:IMSR_JAX: 006440)[53] crossed to a *Pax6::Cre* driver (STOCK Tg(Pax6-GFP/cre)1Rilm/J. Strain #: 024578. RRID:IMSR JAX: 024578. Common Name: P0-3.9GFPCre),[54] as previously described.[47,48,50] To generate *Pten* Rho-cKO animals, animals with a *Pten*^{fl} allele were crossed to a *Rho-Cre* driver line (STOCK Tg(Rho-cre)2Yzl/J. Strain #: 032909, RRID: IMSR PJAX: 032909).[55] Animals were

maintained on a C57BL/6J background (Strain #: 000664. RRID:IMSR_JAX:000664; Common Name: B6). PCR genotyping was performed as described by Jackson Laboratory. Animals were studied at postnatal day (P)21 (*Pten* RPC-cKO $N = 4$, *Pten* Rho-cKO $N = 4$ and wild-type controls $N = 4$), 3 months (*Pten* RPC-cKO $N = 3$, *Pten* Rho-cKO $N = 3$, and wild-type controls $N = 3$), 6 months (*Pten* RPC-cKO $N = 4$, *Pten* Rho-cKO $N = 3$, and wild-type controls $N = 3$), and 12 months (*Pten* RPC-cKO $N = 4$, *Pten* Rho-cKO $N = 4$, and wild-type controls $N = 3$) of age.

Tissue Harvesting and Processing

Mice were euthanized using CO_2 and the eyeballs were dissected out and transferred to 1X-phosphate-buffered saline (PBS) for rinsing before fixation in 4% paraformaldehyde (PFA) in 1X-PBS overnight at 4°C. The eyes were then rinsed in 1X-PBS and immersed in 20% sucrose/1X PBS overnight at 4°C for cryoprotection. The eyes were then embedded in O.C.T. (Tissue-Tek; Sakura Finetek U.S.A. Inc., Torrance, CA, USA) and frozen on dry ice. Embedded eyes were cryosectioned at 10 µm thickness on a Leica CM3050s cryostat (Leica Biosystems, Buffalo Grove, IL, USA) and mounted on Fisherbrand Superfrost Plus slides (Thermo Fisher Scientific, Markham, Ontario, Canada).

Immunostaining

Sectioned tissue was washed in 1X-PBS with 0.1% Triton X-100 (PBST) 3 × 10 minutes at room temperature. Slides were blocked in 10% horse serum in PBST for 1 hour at room temperature before adding primary antibody diluted in 10% horse serum in PBST overnight at room temperature. The slides were then washed for 3 × 10 minutes before incubating in secondary antibodies for 1 hour at room temperature. The slides were washed for 3 × 10 minutes in PBST, counterstained for 5 minutes with DAPI (4′,6-diamidino-2-phenylindole) for 10 minutes, washed for 3 × 10 minutes in PBS, and coverslipped in Aqua-Poly/Mount (Polysciences #18606). Prior to amyloid-β immunostaining, slides were incubated in 70% formic acid for 5 minutes, then transferred to borate buffer (pH = 8.0) for 10 minutes. For amyloid-β (6F/3D), slides were incubated with 10% horse serum with F(ab) anti-mouse IgG fragment (1:500; #ab6668; Abcam Inc.) for 1 hour, and then the slides were rinsed 3 × 5 minutes with PBST. Primary antibodies included: mouse anti-amyloid-β (6F/3D) (1:127 #M0872; DAKO), rabbit anti-ARR3 (1:400, #AB15282; Millipore Sigma), goat anti-GFAP (1:400; #nb-10053809; Novus), rabbit anti-IBA1 (1:400, #019-19741; Fujifilm), mouse anti-RHO (1:400, MAB5356; Millipore Sigma), mouse anti-RPE65 (1:400, clone ID #401.8B11.3D9, SKU TA309839; Origene), and rabbit anti-*PTEN* (138G6; 1:100, #9559; Cell Signaling). The following secondary antibodies were used: donkey anti-mouse IgG Alexa Fluor 555 (#A32773; Invitrogen), donkey anti-rabbit IgG Alexa Fluor 568 (#A10042; Life Technologies), donkey anti-rabbit IgG Alexa Fluor 488 (#21206; Invitrogen), and donkey anti-goat IgG Alexa Fluor 568 (#A11057; Invitrogen).

Histological and Lectin Stains

Diaminobenzidine tetrahydrochloride (DAB) immunohistochemistry was performed using a Vectastain Elite ABC-HRP Peroxidase (Standard) kit (PK-6100; Vector Laboratories), according to the manufacturer's instructions. When the DAB brown precipitate was visible, the slides were rinsed in water, dehydrated in 50% → 70% → 90% → 95% → 100% ethanol baths for 5 minutes each, and immersed in xylene before mounting in Permount Mounting Medium (#17986-01; VWR). For isolectin staining, slides were blocked with 10% horse serum at room temperature for 1 hour. The slides were then incubated in Isolectin GS-IB_4 (Iso-B4) from *Griffonia simplicifolia*, Alexa Fluor 488 Conjugate (1:250; Sigma-Aldrich, Canada). The sections were then washed for 3 × 5 minutes with PBST, counterstained for 5 minutes with DAPI, washed with PBST for 3 × 5 minutes, and coverslipped in AquaPolymount. For PNA staining, sections were blocked for 1 hour in 10% normal goat serum in 1X PBST. Peanut agglutinin (PNA) fluorescein-labeled (NC9014124; Thermo Fisher Scientific, Vector Laboratories) was diluted 1:500 in blocking buffer and incubated on the slides at room temperature overnight. The sections were washed in 3 × 10-minute washes in PBST. The sections were counterstained with DAPI and coverslipped in AquaPolymount.

Rapamycin and 2-deoxy-d-glucose Treatment

Pten RPC-cKO mice were administered rapamycin (2 mg/kg in 0.25% polyethylene glycol [PEG]; 202398; Sigma Aldrich, Canada) and 0.25% Tween-80 (P4780; Sigma Aldrich) in PBS; CAS #53123-88-9; LC Laboratories) or 2-deoxy-d-glucose (2DG; 30 mg/kg in PBS; D3179; Sigma) from P7 to P21 by intraperitoneal injections compared to vehicle control (0.25% PEG/0.25% Tween-80 in PBS). The animals were euthanized and the eyes were dissected out and processed as described.

Lactate Assay

To measure lactate levels, retinas injected with vehicle and 2DG were dissected on ice-cold PBS. Half of the retinas were lysed in 150 uL of RIPA lysis buffer (lab-made, 25 mM Tris•HCl pH 7.6, 150 mM NaCl, 1% NP-40, 1% sodium deoxycholate, 0.1% SDS) with added 1 uM PMSF (#P7626; Sigma-Aldrich) and 25X Complete Protease Inhibitor Cocktail Tablets (#04693116001; Roche). Protein amounts were quantified with a Micro BCA Protein Assay Kit (#23235; ThermoFisher Scientific) following the manufacturer's instructions. Then, the deproteinization step was performed to remove possible present endogenous lactate dehydrogenase in the sample, which might degrade lactate using the Deproteinizing Sample Preparation Kit – TCA (ab204708; Abcam). Measurements of lactate were then performed using an L-Lactate Assay Kit (Colorimetric/Fluorometric) as per the manufacturer's protocol (ab65330; Abcam) and normalized to protein levels.

Bulk RNA-Seq Data Mining

We mined and re-analyzed a previously reported RNA-seq dataset collected from P0 wild-type ($N = 4$) and *Pten* RPC-cKO ($N = 5$) retinas.[43] Genes with low expression (less than one read per million) could not be reliably tested and were removed from the dataset. Differential gene expression was detected using the DESeq2 1.28.1 package. Genes with an adjusted *P* value less than 0.05 (Wald test, Benjamini-Hochberg correction for multiple comparisons) were considered differentially expressed. Over-representation of pathways was determined by the analysis of Gene Ontology

Investigative Ophthalmology & Visual Science

(GO) terms for Biological Process and Kyoto Encyclopedia of Genes and Genomes (KEGG) pathways. Dysregulated pathways were detected using the clusterProfiler 3.16.0 package. KEGG/GO terms with a *P* value of less than 0.05 were considered significantly dysregulated. KEGG/GO pathway analysis was performed for up- and downregulated genes separately. Pathways were visualized using the Pathview 1.28.0 package.

RNA Extraction, cDNA Synthesis, and Quantitative PCR

RNA was isolated from the retinas with RNAeasy Mini Kit (#74104; Qiagen) following the manufacturer's instructions. After which, 450 ng (P0) and 260 ng (12 months) of purified RNA were used for cDNA synthesis using RT^2 First Strand Kit (#330404; Qiagen) following the manufacturer's instructions. cDNA was used to run RT-qPCR using RT^2 SYBR Green qPCR Mastermix (#330501; Qiagen) and mouse primers from Qiagen GeneGlobe: *Pde6b* (#PPM37785A), *Apba2* (PPM25149A), *Dhcr24* (#PPM05205F), *Apoe* (#PPM04128B), *Rp1l1*(#PPM39056A), *Opn1sw* (#PPM29570A), *Cnga3* (#PPM06966A), *Cngb3* (#PPM06965B), *Srebf1* (#PPM05094A), *Rxrg* (#PPM03534A), *Thrb* (#PPM41867F), *Rcvrn* (#PPM31906A), *Fasn* (#PPM03816F), *Apbb2* (#PPM25267A), *Rora* (#PPM03350A), *Nxnl1* (#PPM33435A), *Bsg* (#PPM03834F), *Impg2* (#PPM31707A), *Gnat2* (#PPM06964A), and *B2m* (#PPM03562A), *Gapdh* (#PPM02946E), and *Hprt* (#PPM03559F) as housekeeping genes.

In Vivo Optical Coherence Tomography

For in vivo optical coherence tomography (OCT) imaging, 6-month-old *Pten* RPC-cKO and wild-type control mice were first anesthetized using 2% isoflurane. Pupil dilation was achieved using tropicamide topical drops (Mydriacyl 1%; Alcon Canada Inc., Canada). Live mice were then imaged using both the Spectralis OCT and confocal scanning laser ophthalmoscopy (cLSO) system adapted for mice imaging with a 25-diopter lens (Spectralis OCT + cSLO; Heidelberg Engineering, Germany). Corneas were kept hydrated by applying normal saline every 2 minutes. Fundus scans using infrared cSLO as well as OCT scans were acquired and exported from the native HEYEX software (Heidelberg Engineering, Germany) as tiff images and processed using ImageJ software (NIH, USA). Additionally, colored fundus photographs of both *Pten* RPC-cKO and wild-type mice were acquired using the MICRON IV system (Phoenix; MICRON, CA, USA).

RNA In Situ Hybridization

RNA in situ hybridization was performed using digoxygenin (dig)-labeled *Nxnl1* and *Bsg* antisense probes generated with a Roche – DIG RNA Labeling Mixture (#11277073910 Supply Solutions; SIGMA) according to the manufacturer's instructions. Sections were hybridized with dig-labeled riboprobes in hybridization buffer (50% formamide, 10% dextran sulfate, 1 mg/ml yeast t-RNA, 1 × Denhardt's solution, 1 × salt [0.2M NaCl, 10 mM Tris-HCl pH 7.5, 6.5 mM NaH2PO4, 5 mM EDTA]) and incubated at 65°C in trays humidified with 50% formamide/1 × salt overnight. Probes were washed off with 2 × 30-minute washes in 1 × SSC/50% formamide/0.1% tween 20 at 65°C and then 2 × 30 minutes washes in MABT (100 mM maleic acid, 150 mM NaCl, 0.1% tween 20; pH 7.5). Tissues were blocked in 2% Millipore Sigma Roche Blocking Reagent for Nucleic Acid Hybridization and Detection (#11096176001; SIGMA)/20% normal goat serum/1x MABT and then incubated with a Roche anti-digoxigenin-AP, Fab fragment antibody (#11093274910; Millipore Sigma) at room temperature overnight. Slides were washed 5 × 20 minutes in 1x MABT and 2x in NTMT (100 mM NaCl, 50 mM MgCl2, 100 mM Tris-HCl pH 9.5, 5 mM levamisole). Slides were incubated in alkaline phosphatase-dependent Roche NBT/BCIP stock solution (#11681451001; Millipore Sigma) substrate solution (0.33 mg/mL NBT (Roche) and 0.26 mg/mL BCIP (Roche) diluted in NTMT. After color development, the slides were washed in water, dried overnight, and mounted in Permount Mounting Medium (#17986-01; VWR).

Quantification and Statistical Analysis

To quantify retinal nuclei, either total nuclear numbers or the number of nuclear rows in the ONL, or to quantify cone pedicles a minimum of 3 images from each eye were captured within 800 µm of the optic nerve, in the mid-temporal and mid-nasal retina. For isolectin staining, labeled pixels were quantified in the ONL. For amyloid-β staining, the total number of deposits was calculated from eight different sections for each *N*. One-way ANOVA with Tukey post hoc test was used for statistical analysis comparing three groups, or an unpaired student's *t*-test for two groups (GraphPad Prism, version 9.0.2).

Results

Photoreceptor-Specific Gene Expression Levels Decline in *Pten* RPC-cKO Retinas at Early Postnatal Stages

The prevailing view is that cone photoreceptors die in retinal degenerative diseases due to starvation. Indeed, by deleting *Pten* in cone photoreceptors, mTORC1 signaling is elevated and metabolically challenged cones survive longer in a mouse model of RP.[31] However, the long-term impact of *PTEN* deletion on photoreceptor health, especially in the absence of disease, has not been tested. To first examine the impact of *Pten* loss on photoreceptor health, we analyzed *Pten* RPC-cKOs, in which *Pten* was deleted in RPCs and all progeny neurons, including rod and cone photoreceptors.[43,47–50] In this transgenic model, we previously confirmed that mTORC1 signaling is upregulated.[47,48,50] To assess whether *Pten* loss in embryonic RPCs triggers transcriptomic changes in cell survival pathways and/or photoreceptor-specific gene expression, we mined a bulk RNA-seq dataset collected from P0 *Pten* RPC-cKO retinas and littermate controls.[43] To search for dysregulated pathways, we performed KEGG pathway analysis, identifying 36 significantly enriched pathways ($P < 0.05$), of which 27 were upregulated, including glycolysis.[43] Of the nine KEGG terms associated with a downregulation of gene expression in P0 *Pten* RPC-cKO retinas, several neurodegenerative disease pathways were identified (e.g. Alzheimer's disease, amyotrophic lateral sclerosis, Huntington's disease, etc.; Fig. 1A). These data were consistent with a potential pro-survival impact of *Pten* deletion in the retina.

Previous cellular analyses revealed that *Pten* RPC-cKOs have fewer rod photoreceptors than littermate controls at P7, despite the initial precocious differentiation of photore-

Investigative Ophthalmology & Visual Science

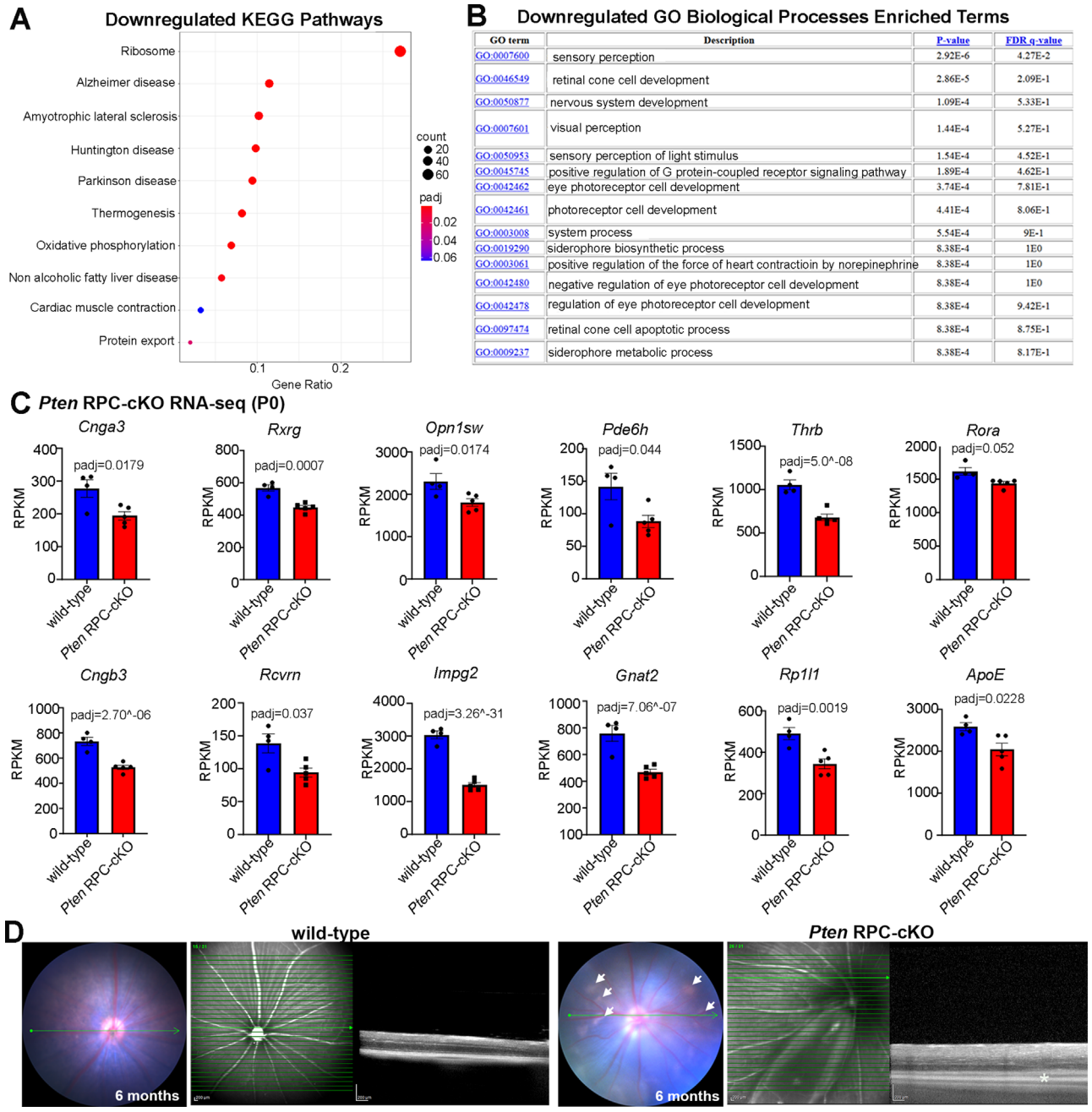

GO term	Description	P-value	FDR q-value
GO:0007600	sensory perception	2.92E-6	4.27E-2
GO:0046549	retinal cone cell development	2.86E-5	2.09E-1
GO:0050877	nervous system development	1.09E-4	5.33E-1
GO:0007601	visual perception	1.44E-4	5.27E-1
GO:0050953	sensory perception of light stimulus	1.54E-4	4.52E-1
GO:0045745	positive regulation of G protein-coupled receptor signaling pathway	1.89E-4	4.62E-1
GO:0042462	eye photoreceptor cell development	3.74E-4	7.81E-1
GO:0042461	photoreceptor cell development	4.41E-4	8.06E-1
GO:0003008	system process	5.54E-4	9E-1
GO:0019290	siderophore biosynthetic process	8.38E-4	1E0
GO:0003061	positive regulation of the force of heart contractioin by norepinephrine	8.38E-4	1E0
GO:0042480	negative regulation of eye photoreceptor cell development	8.38E-4	1E0
GO:0042478	regulation of eye photoreceptor cell development	8.38E-4	9.42E-1
GO:0097474	retinal cone cell apoptotic process	8.38E-4	8.75E-1
GO:0009237	siderophore metabolic process	8.38E-4	8.17E-1

Figure 1. Transcriptomic changes in photoreceptor genes in P0 *Pten* RPC-cKO retinas. (**A**) KEGG pathway analysis of bulk RNAseq data in P0 *Pten* RPC-cKO and wild-type controls. (**B**) GO analysis showing downregulated genes in bulk RNAseq data in *Pten* RPC-cKO and wild-type controls. (**C**) Normalized RPKM (reads per kilobase million) values for *Cnga3*, *Cngb3*, *Opn1sw*, *Pde6h*, *Gnat2*, *Rora*, *Thrb*, *Rxrg*, *Rcvrn*, *Rp1l1*, and *ApoE* in P0 wild-type and *Pten* RPC-cKO retinas. Plots show means ± SEM ($N = 4$ biological replicates for wild-type and $N = 5$ for *Pten* RPC-cKO retinas). Adjusted P values calculated as described. (**D**) Fundus photographs, infrared cSLO fundus images, and OCT scans of wild-type controls and *Pten* RPC-cKO at 6 months of age. *Arrows* in the fundus images and the *asterisk* in the OCT scan denote subretinal deposits. *Scale bars* = 200 µM.

ceptors during the embryonic period,[47] driven in part by an increase in glycolysis.[43] In contrast, cone photoreceptors were present in their proper numbers in P7 *Pten* RPC-cKO retinas.[47] To correlate these findings with transcriptomic changes, we performed GO on the mined RNA-seq dataset.[43] We focused on biological process terms associated with downregulated genes in P0 *Pten* RPC-cKO retinas. Enriched GO terms in the downregulated gene list included "sensory perception," "retinal cone cell development," "visual perception," etc. (Fig. 1B). To determine whether photoreceptor-specific gene expression was indeed perturbed in P0 *Pten* RPC-cKO, we examined reads per kilobase per million mapped reads (RPKM) values as a quantitative measure of transcript levels. RPKM values for genes associated with rod photoreceptor development (*Nr2e3* and *Nrl*) and function (*Rho*) did not reveal any change in gene expression in P0 *Pten* RPC-cKO retinas, suggesting that rod defects have not yet appeared. In contrast, several genes expressed in

Investigative Ophthalmology & Visual Science

cone photoreceptors were downregulated in P0 *Pten* RPC-cKO retinas, including cone photoreceptor nucleotide-gated channels (*Cnga3* and *Cngb3*), the short-wavelength opsin (*Opn1sw*), the cone-specific *Pde6h* subunit of PDE6,[56] and the alpha subunit of cone outer segments (*Gnat2*), mutations in which are observed in patients with achromatopsia[57] (Fig. 1C). Additionally, transcription factors responsible for the fate of different cone photoreceptor subtypes, including *Rora, Rxrg,* and *Thrb*, were downregulated (Fig. 1C). Finally, genes integral to the functions of both rods and cone photoreceptors were also expressed at lower levels in P0 *Pten* RPC-cKO retinas, including *Rcvrn* (Fig. 1C), a calcium-binding protein that plays a significant role in modulating rod phototransduction through enhancing rod sensitivity to dim light.[58] Furthermore, the interphotoreceptor matrix proteoglycan 2 (*Impg2*) was downregulated in P0 *Pten* RPC-cKO retinas (see Fig. 1C), the mutation of which is observed in patients with RP with early macular involvement.[59]

Whereas deleting *Tsc1* in rod photoreceptors rescues cone photoreceptor degeneration in a mouse model of RP,[31] in wild-type mice, *Tsc1* deletion induces AMD-like pathologies.[36] To determine whether *Pten* deletion similarly results in a degenerative phenotype in a wild-type background, we used OCT to take fundus images of 6-month-old wild-type and *Pten* RPC-cKO retinas (Fig. 1D). Clear signs of GA were observed in fundus images of 6-month-old *Pten* RPC-cKO retinas, whereas in the OCT sections, there was a thinning of the ONL, indiscernible bands of inner (IS) and OS segments, and evidence of subretinal deposits (see Fig. 1D).

Taken together, these data suggest that rod photoreceptor differentiation is unperturbed in *Pten* RPC-cKO retinas at P0, whereas cone-specific gene expression is downregulated. However, by 6 month of age, degeneration is evident in the ONL.

Loss of Rod Photoreceptors and Reduced Photoreceptor-Specific Gene Expression Is Recapitulated to a Lesser Extent in Photoreceptor-Specific *Pten* Rho-cKO Mice

The reduction in cone-specific gene expression was unexpected given that the total number of rod photoreceptors is reduced by P7 in *Pten* RPC-cKO retinas, whereas the number of Arr3^{+} cones does not differ.[47] We therefore performed additional analyses of rod and cone photoreceptors in *Pten* RPC-cKO retinas at older ages to better understand the impact of *Pten* deletion on photoreceptor survival. For this purpose, in addition to using RPC-cKOs, we generated a second rod-specific *Pten* deletion using a Rho-Cre driver,[55] hereafter referred to as *Pten* Rho-Cre animals (Fig. 2A). We first examined *PTEN* expression in these models at 12 months of age. In wild-type retinas, high expression of *PTEN* was detected in the GCL, INL, and inner plexiform layer (IPL) and outer plexiform layer (OPL), and lower expression in the ONL and photoreceptor outer segments (Fig. 2B). In 12-month-old *Pten* RPC-cKO retinas, there was a near complete absence of *PTEN* expression throughout the layers in the mid-temporal and mid-nasal retina, where Pax6-Cre is active[54] (see Fig. 2B). Finally, in 12-month-old *Pten* Rho-Cre animals, *PTEN* expression was lost in the ONL and expression in the OSs was sharply reduced, with remaining labeling likely corresponding to cone outer segments (see Fig. 2B).

To assess whether there were signs of retinal degeneration in *Pten* RPC-cKO and *Pten* Rho-Cre retinas at 12 months of age, we immunostained for Rhodopsin (RHO) and labeled nuclei with DAPI. RHO staining was reduced in the OSs of 12-month-old *Pten* RPC-cKO retinas (Fig. 2C), consistent with previous studies demonstrating shortened OSs in *Pten* RPC-specific cKOs.[52] To assess photoreceptor degeneration, we counted the layers of nuclei in the ONL. Typically, there are 11 to 12 rows of photoreceptor nuclei in the ONL of wild-type mice, and our counts confirmed the presence of 11.6 $\pm$ 0.1 nuclear layers in the ONL of 12-month-old wild-type retinas (see Figs. 2C, 2D). In contrast, there were only 7.0 $\pm$ 0.2 and 7.9 $\pm$ 0.1 rows of photoreceptor nuclei in *Pten* RPC-cKO and *Pten* Rho-Cre retinas, respectively. Taken together, these data suggest that by 1 year of age, photoreceptors degenerate in the absence of *Pten* function, irrespective of whether *Pten* is deleted at the RPC stage or specifically deleted in rod photoreceptors.

Finally, we asked whether the same genes associated with photoreceptor function that were downregulated in *Pten* RPC-cKO retinas were also deregulated in *Pten* Rho-cKO retinas. For this purpose, we extracted RNA from P0 wild-type and *Pten* Rho-Cre retinas, and performed qPCR (Fig. 2E). Strikingly, at P0, we observed a reduction in *Cngb3*, *Rcvrn*, *Impg2*, *Gnat2*, and *Rp1l1* expression in *Pten* Rho-Cre retinas, mimicking the defects observed in the RPC-specific cKOs (Fig. 2F). Although not all of the photoreceptor genes that were downregulated in *Pten* RPC-cKOs were affected when *Pten* was deleted in rods (Supplementary Fig. S1), the reduced expression of a subset of photoreceptor genes at P0 suggests that early molecular defects may set the stage for later degeneration. These findings are in keeping with the growing appreciation for the idea that neurodevelopmental changes may increase susceptibility to neurodegenerative disease.[60]

Progressive Photoreceptor Degeneration Following *Pten* Deletion in RPCs and in Rod Photoreceptors

Because aging is a determinant factor for retinal degenerative diseases like AMD,[61] to determine whether *Pten* loss has a progressive impact on photoreceptor survival, we examined photoreceptor numbers in *Pten* RPC-cKO and *Pten* Rho-cKO retinas at a series of stages, including P21, when retinal cell differentiation is complete, and at 3, 6, and 12 months of age, after the developmental window (Fig. 3). To monitor photoreceptor number, we quantified DAPI^{+} nuclei in the ONL, focusing on the mid-temporal and mid-nasal retina because the Pax6-cre driver is not active in a central, dorsomedial wedge.[47,48,50,54] Consequently, whereas *PTEN* immunolabeling extends across the wild-type retina, *PTEN* is only expressed in the medial retina adjacent to the optic nerve head in *Pten* RPC-cKO retinas (see Fig. 3A). Thus, nuclear counts on mid-nasal and mid-temporal areas that were 800 µm from the optic nerve head (see Figs. 3B, 3C).

At P21, a 1.2-fold reduction in ONL cell number was observed in *Pten* RPC-cKO retinas, which became more apparent over time, with 1.3-fold, 1.9-fold, and 2.3-fold reductions in ONL nuclei observed at 3, 6, and 12 months of age, respectively (see Figs. 3D, 3E). In contrast, in *Pten* Rho-cKO animals, a decline in ONL nuclei was not observed until 6 months of age (1.3-fold decline), worsening by 12 months to be as severe as the *Pten* RPC-cKO retinas (2.2-fold decline; see Figs. 3D, 2E). Because rods represent 97% of all photore-

Investigative Ophthalmology & Visual Science

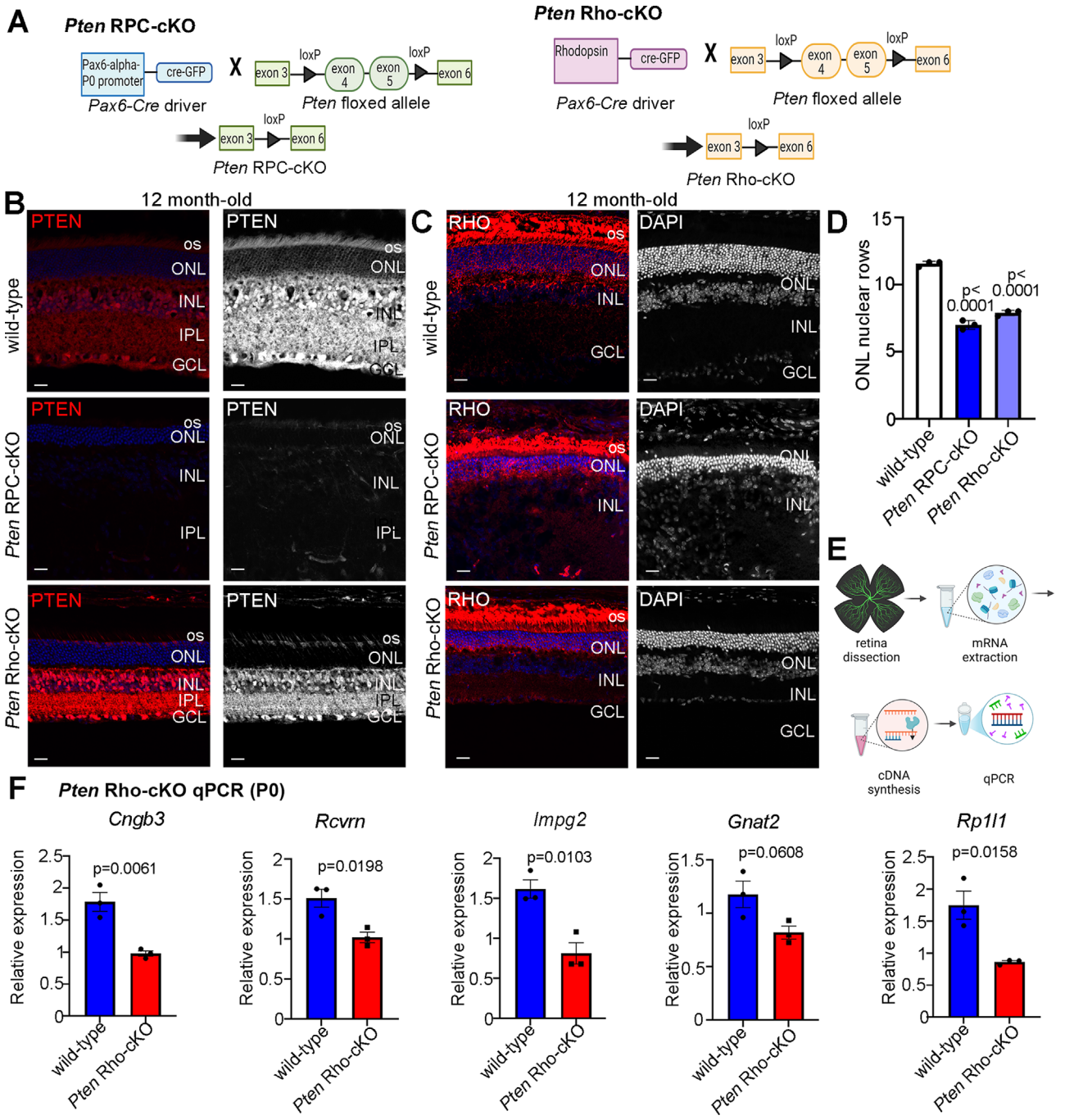

Figure 2. Generation and characterization of *Pten* RPC-cKO mice and *Pten* Rho-cKO mice. (**A**) Schematic showing the generation of *Pten* RPC-cKO and *Pten* Rho-cKO mice. (**B**) Immunolabeling of 12-month-old wild-type, *Pten* RPC-cKO and *Pten* Rho-cKO retinas with *PTEN*. (**C**) Immunolabeling of 12-month-old wild-type, *Pten* RPC-cKO and *Pten* Rho-cKO retinas with Rhodopsin (RHO) and a DAPI nuclear stain. (**D**) Graph and statistical analysis of ONL nuclear rows in wild-type, *Pten* RPC-cKO, and *Pten* Rho-cKO retinas at 12 months of age ($N = 3$ each). (**E**) Schematic representation of retinal dissection, mRNA extraction, cDNA synthesis, and qPCR. (**F**) qPCR analysis of *Cngb3*, *Rcvrn*, *Impg2*, *Gnat2*, and *Rp1l1* in P0 wild-type and *Pten* Rho-cKO retinas ($N = 3$ each). Plots show means ± SEM in all plots. The *P* values calculated with 1-way ANOVA with Tukey post hoc test (**D**) or unpaired *t*-test (**F**). GCL, ganglion cell layer; INL, inner nuclear layer; ONL, outer nuclear layer; os, outer segments. *Scale bar* = 10 µm.

ceptors in rodent retinas,[1,2] ONL counts were mainly rod photoreceptors. The decline in photoreceptor number was not accompanied by any changes in the total number of DAPI$^+$ nuclei in the GCL + INL in either *Pten* RPC-cKO or in *Pten* Rho-cKO retinas at P21, and 3 and 6 months of age (see Figs. 3D, 3E). However, by 12 months of age, *Pten* Rho-cKO animals also had a slight decline in GCL + INL cells (see Figs. 3D, 3E).

These data are consistent with a progressive thinning of the ONL in both *Pten* RPC-cKO and *Pten* Rho-cKO retinas. However, the loss of rod photoreceptors is accelerated and more severe in *Pten* RPC-cKO mice, suggest-

Investigative Ophthalmology & Visual Science

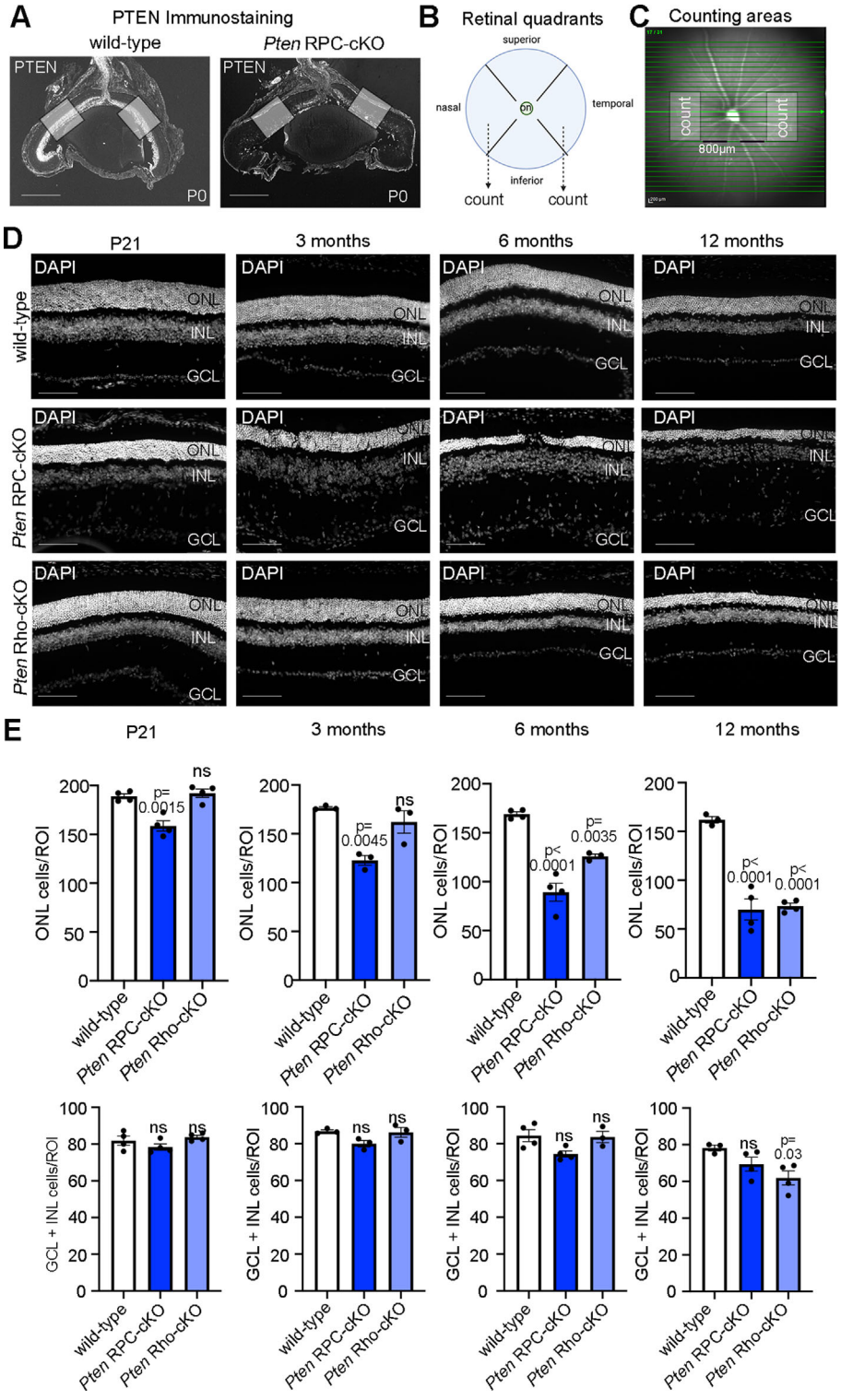

Figure 3. Progressive photoreceptor degeneration in *Pten* cKO retinas. (**A**) *PTEN* immunolabeling of P0 wild-type and *Pten* RPC-cKO retinas. The *boxed areas* show a region of cell counts. (**B**) Schematic of retinal quadrants, showing that counts were conducted in the mid-nasal and mid-temporal regions away from the optic nerve head. (**C**) Fundus photograph of 6-month-old wild-type retina, showing the region of cell counts at 800 µm from the optic nerve head. (**D**) Retinal cross sections showing ONL and GCL/INL thickness at P21, 3, 6, and 12 months of age in wild-type, *Pten* RPC-cKO, and *Pten* Rho-cKO retinas. (**E**) Plots show means ± SEM in all plots. P21: wild-type ($N = 4$), *Pten* RPC-cKO ($N = 4$), and *Pten* Rho-cKO ($N = 4$), 3 months: wild-type ($N = 3$), *Pten* RPC-cKO ($N = 3$), and *Pten* Rho-cKO ($N = 3$), 6 months: wild-type ($N = 4$), *Pten* RPC-cKO ($N = 4$), and *Pten* Rho-cKO ($N = 3$) and 12 months: wild-type ($N = 3$), *Pten* RPC-cKO ($N = 4$), and *Pten* Rho-cKO ($N = 4$) with 3 technical replicates. The *P* values calculated with 1-way ANOVA with Tukey post hoc test. GCL, ganglion cell layer; INL, inner nuclear layer; ONL, outer nuclear layer. *Scale bars* = 200 µM in **C** and 100 µm in **D**.

Investigative Ophthalmology & Visual Science

ing that the loss of *Pten* in other retinal cells contributes to the degenerative phenotype. Photoreceptor survival is maintained by the RPE, which provides photoreceptors with growth factors and nutrients, recycles photopigments, and phagocytoses photoreceptor outer segments.[62] *Pten* is expressed at high levels in the RPE, and an RPE-specific *Pten* cKO results in RPE cell dysfunction due to an epithelial-to-mesenchymal transition and photoreceptor degeneration from P8.[63] However, RPE defects are unlikely to be the initial trigger for photoreceptor degeneration in *Pten* RPC-cKOs as the RPE is intact in these mice at P21 (Supplementary Figs. S2A, S2B).

Cone Photoreceptors Progressively Degenerate in *Pten* RPC-cKO Retinas

Rods promote cone survival by secreting rod-cone viability factor (RdCVF), encoded by *Nucleoredoxin-like 1* (*Nxnl1*).[64] RdCVF binds a Basigin (*Bsg*) receptor to induce aerobic glycolysis and prevent oxidative stress in cones.[64] Both *Nxnl1* and *Bsg* are expressed in P0 *Pten* RPC-cKOs, albeit with a slight reduction in *Nxnl1* transcript counts (see Supplementary Figs. S2C–E). To study the effect of *Pten* loss on cone photoreceptors, we quantified the number of cone pedicles expressing cone arrestin ($Arr3^+$) in the mid-temporal and mid-nasal regions. By P21, a 1.2-fold reduction in cone pedicles was observed in *Pten* RPC-cKOs, which declined even further by 3 months (1.4-fold), 6 months (1.9-fold), and 12 months (2.3-fold) of age (Figs. 4A, 4B). In contrast, *Pten* Rho-cKO retinas did not show a significant change in the number of $Arr3^+$ pedicles at any stage (see Figs. 4A, 4B), despite the overall thinning of the ONL (see Fig. 3). The presence of ARR3 expression in the ONL at 12 months of age is consistent with the ectopic expression of M-cone opsin in the ONL in *Pten* RPC-cKOs from a separate study.[52] To further examine cone defects, we labeled the OSs with peanut agglutinin (PNA). When compared with wild-type retinas, a clear shortening of the PNA-labeled outer segments was observed in both 12 month old *Pten* RPC-cKO and *Pten* Rho-cKO retinas (Fig. 4C).

Taken together, these data suggest that the remaining rod photoreceptors in *Pten* Rho-cKO, which are at approximately 50% of wild-type levels at 12 months of age, are sufficient to support cone survival. In contrast, the loss of cones in *Pten* RPC-cKO retinas may be due in part to developmental changes in cone photoreceptor gene expression (see Fig. 1), and/or the deletion of *Pten* in other retinal cells might be contributing to this pathology.

Signs of Reactive Gliosis and Microglial Activation in *Pten* RPC-cKO and *Pten* Rho-cKO Retinas

In mammals, Müller glia respond to injury by undergoing reactive gliosis, a neuroprotective response that limits cell damage, but which can be cytotoxic when severe.[65] Glial fibrillary acidic protein (GFAP) is a marker of reactive gliosis and is upregulated in rodent models of several retinal pathologies[66] and in the retinas of patients with AMD.[67] Gliosis initially protects neurons and promotes repair,[68,69] but when prolonged can worsen degeneration and result in the formation of gliotic scars.[70] In wild-type retinas at P21, and at 3, 6, and 12 months of age, GFAP expression was only detected at elevated levels in astrocytes lining the GCL and not in the retina proper (Fig. 5A). In *Pten* RPC-cKO retinas, GFAP expression was upregulated in Müller glia spanning the retina and extending to the apical surface of the ONL as early as P21 ($N = 4/4$ retinas; Fig 5B). Furthermore, hypertrophy of Müller glia was evident, with GFAP expression detected in the subretinal space. The increase in GFAP expression increased over time and was associated with the convergence of fibers to form a gliotic scar (see Fig. 5B).

In *Pten* Rho-cKO retinas, increased GFAP immunoreactivity was observed in the INL only at 3 months ($N = 3/3$), which increased by 6 months ($N = 3/3$) and 12 months ($N = 4/4$) of age, but the $GFAP^+$ Müller glial fibers remained in a parallel distribution and did not show the same extent of disorganization or gliotic scar formation as in *Pten* RPC-cKOs (Fig. 5C). $IBA1^+$ microglia were also observed to infiltrate the subretinal space in *Pten* RPC-cKOs from P21, and in *Pten* Rho-cKOs from 6 months of age. Thus, hallmarks of retinal inflammation are observed in both *Pten* RPC-cKO and *Pten* Rho-cKO retinas, but macroglial and microglial phenotypes are much more severe in *Pten* RPC-cKOs. Taken together, these data are suggestive of a role for *Pten* in Müller glia, but more importantly, support the idea that widespread inflammatory signals may contribute to photoreceptor degeneration in the absence of *Pten* function.

Aberrant Angiogenesis in the ONL in *Pten* RPC-cKO and *Pten* Rho-cKO Retinas

Pten-cKO retinas mimic several features of AMD, including photoreceptor degeneration, and microglial and macroglial activation; however, AMD is a multifactorial disorder affecting multiple retinal elements, including the vasculature.[71] Choroidal neovascularization (CNV) is a pathological disease feature in wet AMD, whereas vascular attenuation is observed in patients with RP and vascular regression is seen in RP mouse models.[72,73] *Pten* is known to inhibit angiogenesis and the expression of vascular endothelial growth factor (VEGF), a pro-angiogenic factor.[74] To examine the retinal vasculature, we labeled retinas with Isolectin-B4. In wild-type retinas at P21, and at 3, 6, and 12 months of age, Isolectin-B4 (Iso-B4) labeled 3 vascular plexi in the inner retina, including a superficial (s) plexus (at the GCL level), intermediate (i) plexus (at the inner plexiform layer, or IPL level), and a deep (d) plexus (at the outer plexiform layer, or OPL level; Figs. 6A, 6D). Notably, no Iso-B4 staining was observed in the ONL at any stage in the wild-type retina. In contrast, in *Pten* RPC-cKO retinas, Iso-B4 labeling was observed in the ONL beginning at P21 and throughout 12 months of age (see Figs. 6B, 6D). *Pten* Rho-cKO retinas did not show any Iso-B4 staining the ONL at P21 ($N = 4/4$; see Figs. 6C, 6D). However, Iso-B4 staining in the ONL was observed at 3 months ($N = 3/3$), 6 months ($N = 2/3$), and 12 months ($N = 4/4$; see Figs. 6C, 6D). These data are consistent with the idea that there is aberrant angiogenesis when *Pten* is deleted in RPCs and when deleted in photoreceptors alone.

Increased Lipid Biogenesis Gene Expression and Amyloid-β Subretinal Deposit Formation in *Pten* RPC-cKOs

In dry AMD, lipid and protein deposits known as drusen form between the RPE and Bruch's membrane.[75–77] Because

Investigative Ophthalmology & Visual Science

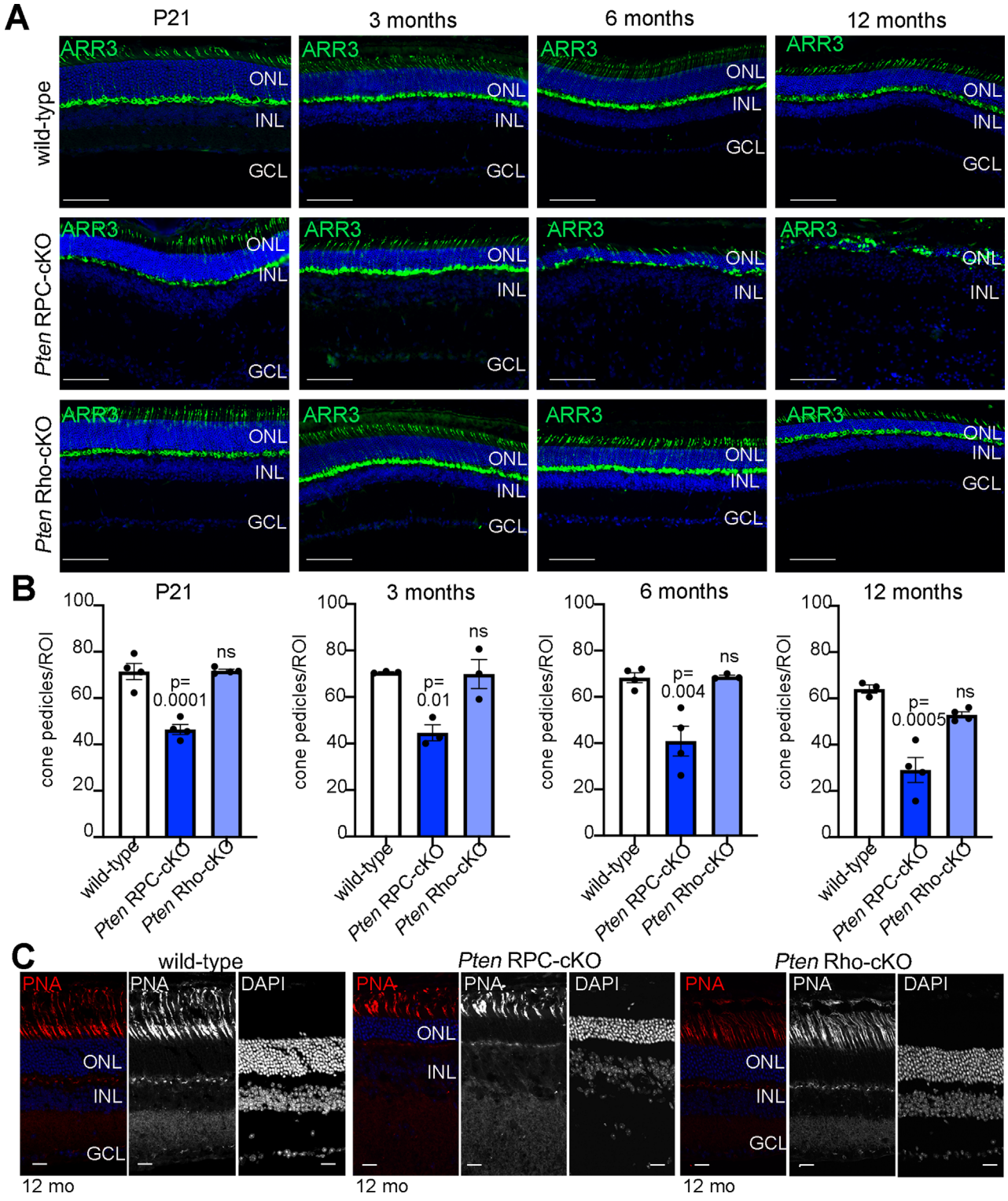

Figure 4. Cone photoreceptor degeneration in *Pten* RPC-cKO retinas at P21. (**A**) Wild-type, *Pten* RPC-cKO, and *Pten* Rho-cKO retinal cross-sections immunostained with ARR3 (*green*) at P21, 3, 6, and 12 months of age. (**B**) Graphs and statistical analysis of the number of ARR3^{+} pedicles in wild-type, *Pten* RPC-cKO, and *Pten* Rho-cKO at P21, 3, 6, and 12 months of age. Plots show means ± SEM in all plots. P21: wild-type ($N = 4$), *Pten* RPC-cKO ($N = 4$), and *Pten* Rho-cKO ($N = 4$), 3 months: wild-type ($N = 3$), *Pten* RPC-cKO ($N = 3$), and *Pten* Rho-cKO ($N = 3$), 6 months: wild-type ($N = 4$), *Pten* RPC-cKO ($N = 4$), and *Pten* Rho-cKO ($N = 3$), and 12 months: wild-type ($N = 3$), *Pten* RPC-cKO ($N = 4$), and *Pten* Rho-cKO ($N = 4$) with 3 technical replicates. (**C**) The 12-month-old wild-type, *Pten* RPC-cKO, and *Pten* Rho-cKO retinal cross-sections labeled with PNA. The *P* values calculated with 1-way ANOVA with Tukey post hoc test. GCL, ganglion cell layer; INL, inner nuclear layer; ONL, outer nuclear layer. *Scale bar* = 100 µm in **A** and 10 µm in **C**.

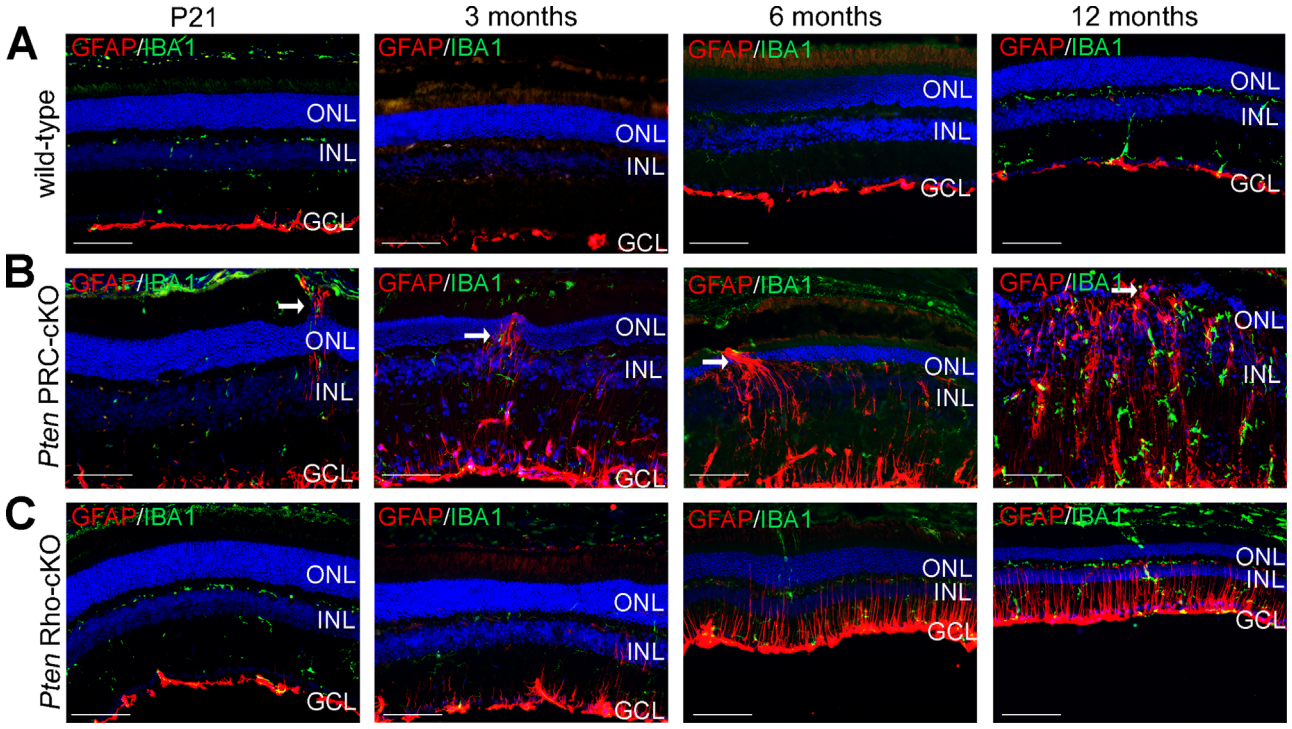

Figure 5. Increased GFAP and microglia activation in *Pten* RPC-cKO and *Pten* Rho-cKO retinas. (**A**) Wild-type retinal cross sections stained with IBA1 (*green*) and GFAP (*red*) from P21 to 12 months of age. (**B**) *Pten* RPC-cKO retinal cross sections stained with IBA1 (*green*) and GFAP (*red*) with subretinal gliosis (*arrow*) from P21 to 12 months of age. The *arrows* denote the glial scarring. (**C**) *Pten* Rho-cKO retinal cross sections stained with IBA1 (*green*) and GFAP (*red*) at P21, 3, 6, and 12 months of age with increased GFAP expression (*asterisk*) at 3, 6, and 12 months of age. The *asterisk* denotes the increased GFAP expression. GCL, ganglion cell layer; INL, inner nuclear layer; ONL, outer nuclear layer. *Scale bar* = 100 µm.

Pten deletion leads to lipid accumulation in different cell types,[78] we asked whether the loss of *Pten* similarly influences lipid biogenesis in the retina. To address this question, we first mined the RNA-seq dataset collected from P0 *Pten* RPC-cKO retinas for lipid synthesis and metabolic genes, revealing an upregulation of key genes, such as *24-dehydrocholesterol reductase* (*Dhcr24*), *Fatty acid synthase* (*Fasn*), and *Sterol regulatory element-binding transcription factor 1* (*Srebf1*; Fig. 7A). *Srebf1* encodes a transcription factor that binds sterol regulatory element-1 (SRE1) in genes that control lipid and cholesterol production. Cholesterol is a central driver of neurodegeneration, contributing to amyloid-β toxicity,[79] which is present in drusen in AMD.[77] We therefore also examined the expression of genes related to amyloid-β, revealing that *Amyloid-β A4 precursor binding protein family A* (*Apba2*) and *Amyloid-β A4 precursor binding protein family B* (*Apbb2*) transcript levels were elevated in P0 *Pten* RPC-cKO retinas (see Fig. 7A). Notably, qPCR analysis of P0 *Pten* Rho-cKO retinas revealed a similar upregulation of *Dhcr24, Srefb1*, and *Apba2* expression (Fig. 7B).

To determine whether the elevated lipid biogenesis and amyloid-related gene expression in *Pten* RPC-cKO retinas at early postnatal stages translated to the formation of retinal lipid deposits, we examined amyloid-β deposits.[80] At P21, wild-type, *Pten* RPC-cKO, and *Pten* Rho-cKO did not show deposits immunoreactive to the amyloid-β antibody, 6F/3D (Figs. 7C, 7D). Wild-type and *Pten* Rho-cKO retinas remained devoid of amyloid-β deposits at all stages analyzed, whereas 6F/3D immunostaining was detected in 3, 6, and 12 months old *Pten* RPC-cKO retinas (see Figs. 7C, 7D).

mTORC1 Inhibition Exacerbates Photoreceptor Degeneration in *Pten* RPC-cKOs

The mTORC1 serves as a nutrient sensor that coordinates cellular demand with nutrient availability by promoting glycolysis. Because mTORC1 signaling is upregulated in several diseases of aging, inhibiting this signaling pathway or its downstream consequences on glycolysis, has been proposed as an anti-aging and pro-regenerative approach.[81] We asked whether the elevation of mTOR and glycolysis in *Pten* RPC-cKO contributes to photoreceptor degeneration by asking if we could rescue this phenotype by inhibiting mTOR or glycolysis in *Pten* RPC-cKO animals. For this purpose, P7 *Pten* RPC-cKO mice were administered rapamycin or 2DG via daily intraperitoneal injections between P7 and P21 (Fig. 8A). Rapamycin is a pharmacological inhibitor of mTORC1, which preserves photoreceptor health in a drug-induced model of RP.[37] The 2DG is an analog of glucose that blocks glycolysis, the effects of which we confirmed by demonstrating a reduction in lactate production in the retina (Fig. 8B). We investigated the impact on photoreceptors by immunolabeling retinas with RHO, a marker of rod photoreceptors, and ARR3 and PNA, cone photoreceptor markers (Fig. 8C). Cone outer segments appeared more disorganized after rapamycin treatment of *Pten* RPC-cKO mice (see Fig. 8C). Furthermore, an investi-

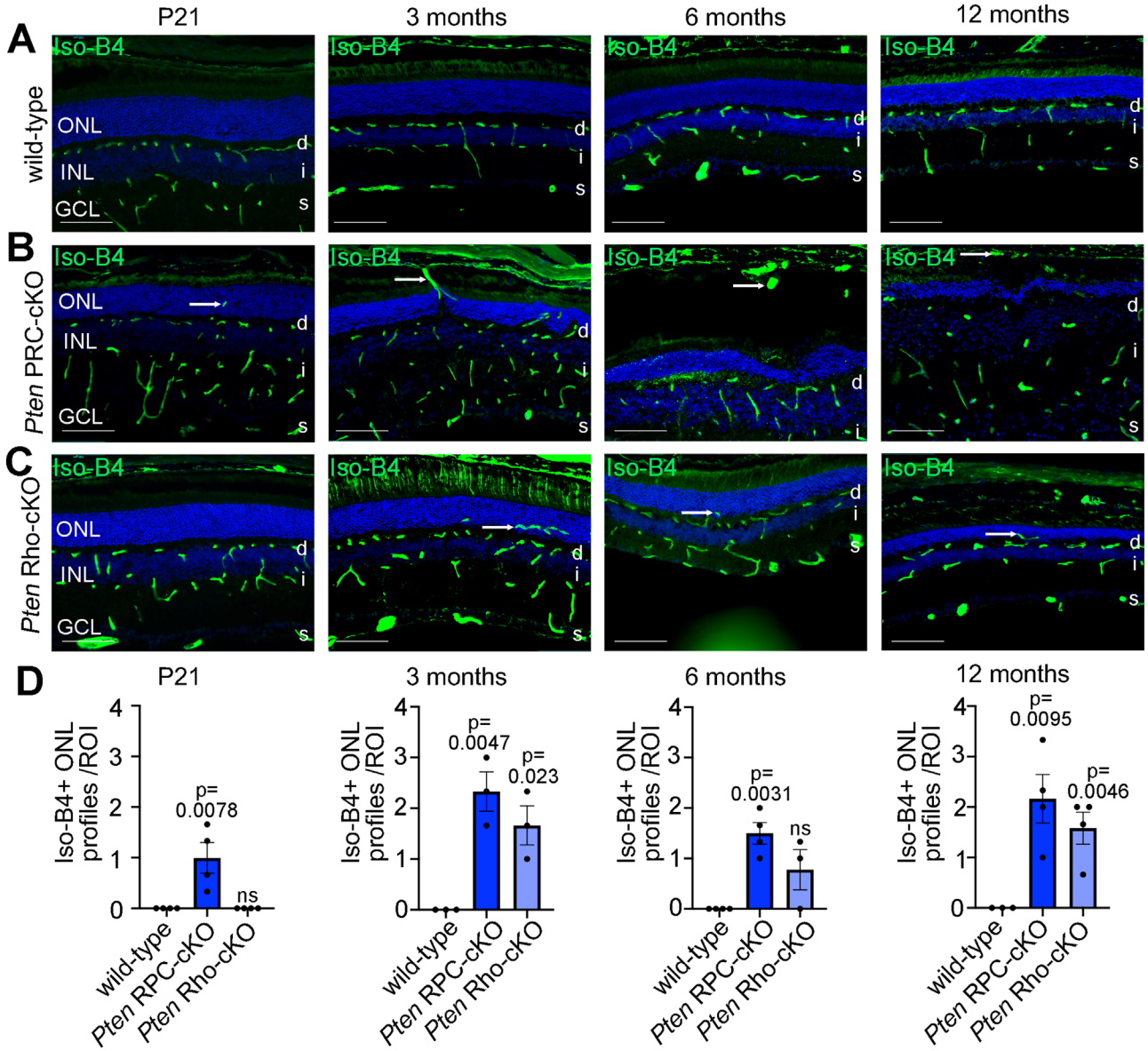

Figure 6. Aberrant angiogenesis in *Pten* RPC-cKO and *Pten* Rho-cKO retinas. (**A**) Wild-type retinal cross section showing isolectin (*green*) staining outlining vascular plexi at P21, 3, 6, and 12 months of age. (**B**) *Pten* RPC-cKO retinal cross section isolectin staining (*green*) showing profiles positive for isolectin staining in the ONL (*arrow*) at P21, 3, 6, and 12 months of age. The *arrows* denote the profiles positive for isolectin in ONL. (**C**) Retinal cross section of *Pten* Rho-cKO showing isolectin staining (*green*) outlining the vascular plexi showing profiles positive for isolectin staining in the ONL (*arrow*) at 3, 6, and 12 months of age. The *arrows* denote profiles positive for isolectin in ONL. (**D**) Graphs and statistical analysis of the number of isolectin+ profiles in the ONL in wild-type, *Pten* RPC-cKO, and *Pten* Rho-cKO at P21, 3, 6, and 12 months of age. Plots show means ± SEM in all plots. P21: wild-type ($N = 4$), *Pten* RPC-cKO ($N = 4$) and *Pten* Rho-cKO ($N = 4$), 3 months: wild-type ($N = 3$), *Pten* RPC-cKO ($N = 3$), and *Pten* Rho-cKO ($N = 3$), 6 months: wild-type ($N = 4$), *Pten* RPC-cKO ($N = 4$), and *Pten* Rho-cKO ($N = 3$) and 12 months: wild-type ($N = 3$), *Pten* RPC-cKO ($N = 4$), and *Pten* Rho-cKO ($N = 4$) with 3 technical replicates. The *P* values calculated with 1-way ANOVA with Tukey post hoc test. GCL, ganglion cell layer; INL, inner nuclear layer; ONL, outer nuclear layer. s: superficial vascular plexus, i: intermediate vascular plexus, d: deep vascular plexus. *Scale bar* = 100 µm.

gation of the ONL cell number revealed that the inhibition of mTORC1 signaling exacerbated the degenerative phenotype associated with *Pten* loss, with a reduction in the number of ONL cells and ONL nuclear layers compared with vehicle controls (Fig. 8D). The OSs also appear shorter upon rapamycin treatment of *Pten* RPC-cKO mice (see Fig. 8C). In contrast, using the same in vivo treatment paradigm to deliver 2DG to inhibit glycolysis had no effect on ONL cell number, ONL nuclear rows, or outer segment morphology in *Pten* RPC-cKO mice (see Figs. 8C, 8D). Together, these data suggest that while photoreceptor degeneration is associated with a loss of *Pten* function, mTORC1 signaling and glycolysis may not be the triggering factors.

Discussion

Despite advances in gene therapies and optogenetics, the treatment of retinal degenerative diseases remains challenging, due in part to disease heterogeneity and the lack of new neuron production after development is complete.[82,83]

Investigative Ophthalmology & Visual Science

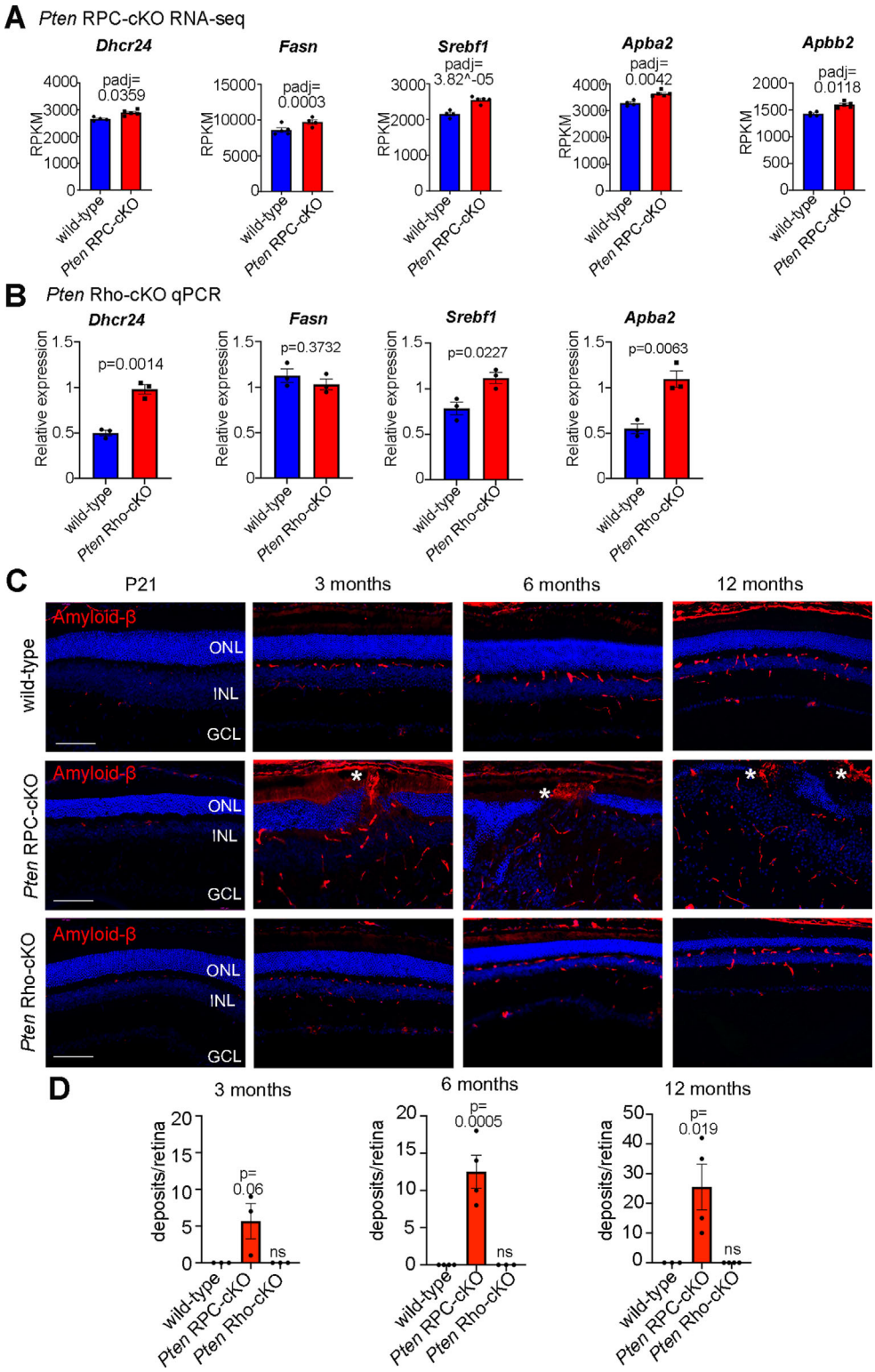

Figure 7. Subretinal amyloid-β deposits develop in *Pten* RPC-cKO retinas. (**A**) Bulk RNA-seq data showing expression of *24-dehydrocholesterol reductase* (*Dhcr24*), *Fatty acid synthase* (*Fasn*), and *Sterol regulatory element-binding transcription factor 1* (*Srebf1*), *Amyloid-β A4 precursor binding protein family A* (*Apba2*), and *Amyloid-β A4 precursor binding protein family B* (*Apbb2*) in wild-type and *Pten* RPC-cKO retinas. (**B**) The qPCR analysis of *Dhcr24*, *Fasn*, *Srebf1*, and *Apba2* in P0 wild-type and *Pten* Rho-cKO retinas ($N = 3$ each). Plots show means ± SEM. (**C**) Wild-type, *Pten* RPC-cKO, and *Pten* Rho-cKO retinal cross sections stained with 6F/3D amyloid-β immunostaining at P21, 3, 6, and 12 months of age. (**D**) Graphs and statistical analysis of the number of 6F/3D amyloid-β+ profiles in the ONL and subretinally in wild-type, *Pten* RPC-cKO, and *Pten* Rho-cKO at 3, 6, and 12 months of age. Plots show means ± SEM in all graphs. For 3 months: wild-type ($N = 3$), *Pten* RPC-cKO ($N = 3$), and *Pten* Rho-cKO ($N = 3$), 6 months: wild-type ($N = 4$), *Pten* RPC-cKO ($N = 4$), and *Pten* Rho-cKO ($N = 3$), and 12 months: wild-type ($N = 3$), *Pten* RPC-cKO ($N = 40$,) and *Pten* Rho-cKO ($N = 4$) with 3 technical replicates. The values were calculated with an unpaired *t*-test (**B**) or 1-way ANOVA with Tukey post hoc test (**D**). GCL, ganglion cell layer; INL, inner nuclear layer; ONL, outer nuclear layer. Scale bar = 100 µm.

Investigative Ophthalmology & Visual Science

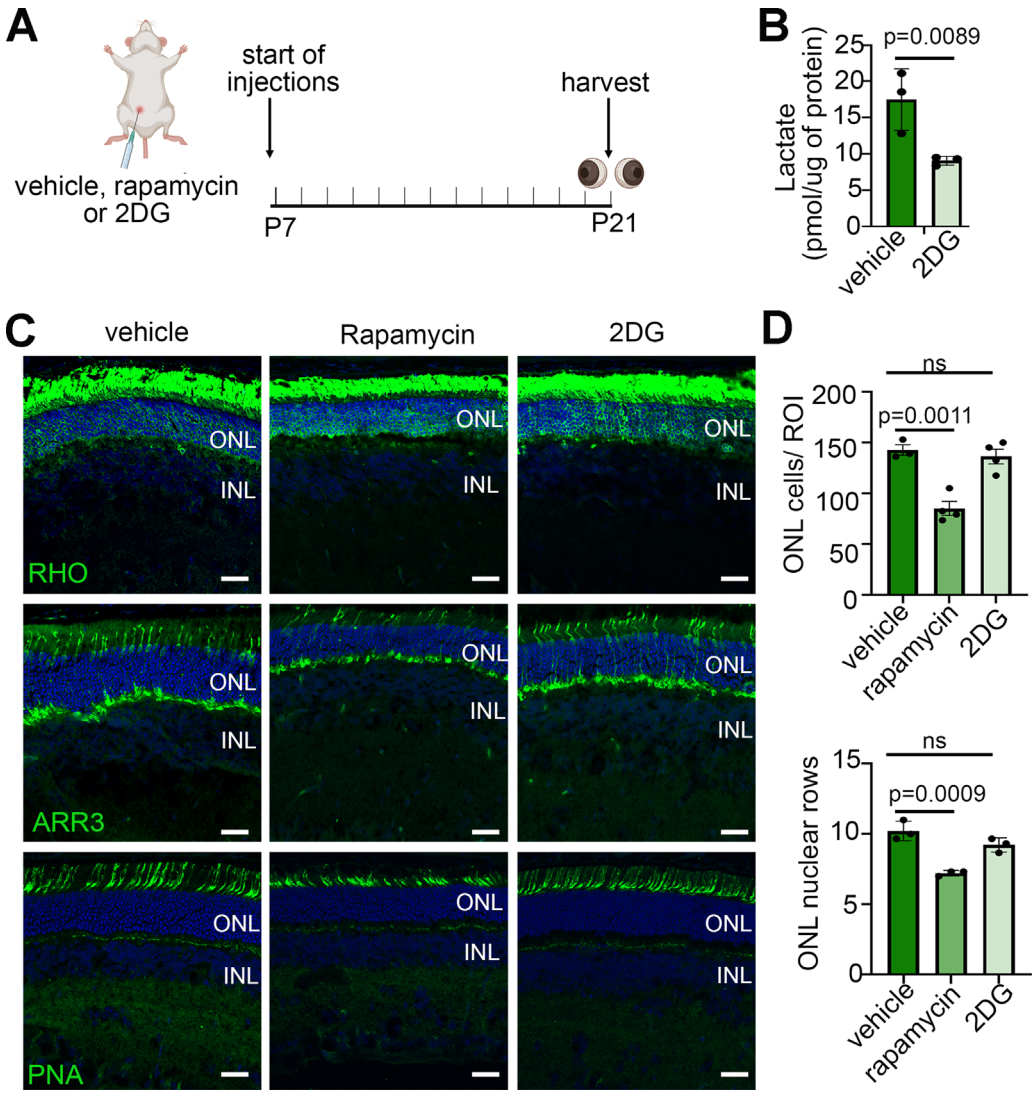

Figure 8. Rapamycin, an mTOR inhibitor, accelerates photoreceptor degeneration in *Pten* RPC-cKO retinas. (**A**) Schematic illustration of P7 *Pten* RPC-cKO mice treated with rapamycin, 2DG, or vehicle control from P7 to P21. (**B**) Measurement of lactate levels in P21 retinas of WT mice treated with 2DG ($N = 3$) and vehicle as a control ($N = 3$). Plot shows mean ± SEM. (**C**) Retinal cross-sections from vehicle, rapamycin, and 2DG treated *Pten* RPC-cKO mice labeled with RHO, ARR3, and PNA. (**D**) Graph and statistical analysis of the number of ONL nuclei and ONL nuclear rows in *Pten* RPC-cKO mice treated with vehicle, rapamycin, and 2DG. Plots show means ± SEM in all graphs. Vehicle ($N = 3$), rapamycin ($N = 3$), and 2DG ($N = 3$). The *P* values calculated with unpaired *t*-test **B** and 1-way ANOVA with Tukey post hoc test **D**. GCL, ganglion cell layer; INL, inner nuclear layer; ONL, outer nuclear layer. *Scale bar* = 25 µm.

Therefore, new animal models are required to better understand disease pathogenesis and to serve as platforms for the testing of novel therapeutics. Notably, *Pten* inhibition promotes axonal regeneration, including in the retina,[45] but the impact of *Pten* loss on retinal cell health and survival over the long-term has yet to be examined. In this study, we examined how *Pten* deletion affects photoreceptor survival in the absence of additional neurodegenerative signals, comparing *Pten* RPC-cKO and *Pten* Rho-cKO mice. We found that rod and cone photoreceptors degenerate rapidly in *Pten* RPC-cKO retinas, accompanied by subretinal deposit formation and the appearance of other retinal pathologies, including macroglia and microglia activation and aberrant vasculature formation in the ONL. In *Pten* Rho-cKO retinas, rod degeneration, macroglia and microglia activation, and aberrant angiogenesis are also observed, albeit at later stages and in less severe forms, whereas amyloid-β deposits do not form. Furthermore, even upon the loss of 50% of rods, cone photoreceptors survive in *Pten* Rho-cKO retinas.

The loss of photoreceptors in *Pten*-cKO retinas is progressive and is likely to have functional consequences on vision in the long-term. We and one other group have previously performed full field ERG recordings on *Pten* RPC-cKO animals.[50,52] At 3 months of age, photoreceptor (a-wave) amplitudes and implicit times are not altered in *Pten* RPC-cKO retinas under scotopic and photopic adaptation.[50,52] However, because ERGs record massed potential across the entire retina, typically more than 20% of photoreceptors must be lost for defects to be measured. At 3 months of age, photoreceptor loss has not yet reached these threshold levels in *Pten* RPC-cKO retinas. Nevertheless, it is anticipated that ERG recordings on older *Pten* RPC-cKO animals would show a-wave defects, in accordance with the progressively

more severe loss of photoreceptors at 6 months of age and later.

Intriguingly, *Pten* RPC-cKO retinas recapitulate many of the pathological features of AMD, including photoreceptor degeneration, GFAP upregulation, and the formation of subretinal deposits that are positive for amyloid-β. GFAP is upregulated in the retinas of patients with AMD[67] and other rodent models of retinal disease.[66] GFAP upregulation is protective initially and promotes repair.[68,69] However, prolonged gliosis ultimately results in the formation of a gliotic scar.[70] In *Pten* RPC-cKO retinas, we observed elevated GFAP expression in Müller glia that spanned the full retinal thickness, with $GFAP^+$ fibers converging to form gliotic scars. This "scarring" was not observed in *Pten* Rho-cKO retinas, in which GFAP expression was elevated, yet Müller glia fibers retained their parallel organization.

What is the significance of the amyloid-β deposits? In AMD, amyloid-β is found in drusen deposits that have been implicated in pathogenesis.[84,85] The idea that the environment is toxic due to these deposits in the AMD retina is consistent with the example of macular translocation in patients with AMD, which results in the recurrence of GA in the new site.[86,87] Additionally, studies in patients with AMD found that the distribution of subretinal deposits and soft drusen matched the regions where rods and cone degeneration were observed.[88,89] Drusen volume is thus an indicator of AMD disease progression,[90] and amyloid-β may be a pathogenic component of this drusen. However, we only observed amyloid-β deposit formation in *Pten* RPC-cKO retinas at 3 months of age and onward, whereas photoreceptor degeneration was evident as early as P21. Furthermore, no amyloid-β deposits were observed in *Pten* Rho-cKO retinas, suggesting that these deposits arise from deleting *Pten* in all retinal cell types, rather than just in rods. Thus, subretinal deposit formation may not be an initial trigger or direct contributor to photoreceptor death, even though it is a pathological feature.

Photoreceptors receive their oxygen and nutrient supply through the choroidal vasculature, which undergoes pathological changes in neurodegenerative diseases. Choroidal neovascularization is observed in patients with AMD and vasculature attenuation is observed in patients with RP.[71–73] In this study, we found evidence of new angiogenesis in the ONL in *Pten* RPC-cKO retinas, where photoreceptors reside, beginning as early as P21. Similarly, *Pten* Rho-cKO retinas also showed signs of angiogenesis in the ONL, but only starting at 3 months of age, preceding photoreceptor degeneration at 6 months. The appearance of aberrant angiogenesis in *Pten* Rho-cKO retinas is suggestive of a crosstalk between photoreceptors and inner retinal vasculature, which may be further addressed in the future.

The mTORC1 complex, which includes the mTOR kinase and Raptor (Rptor) adaptor protein, is a central metabolic regulator, the activity of which is enhanced in the retina in response to *Pten* loss.[47,48] We thus asked whether elevated mTORC1 activity in the absence of *Pten* contributes to photoreceptor degeneration. For this purpose, we inhibited mTORC1 activity in *Pten* RPC-cKO retinas using rapamycin, which was administered from P7 to P21. Strikingly, we found that rapamycin treatment worsened photoreceptor degeneration in *Pten* RPC-cKOs, suggesting that mTORC1 activity may be protective for photoreceptors. Similar findings were reported using a genetic model, wherein deleting *Rptor;Rictor* to reduce mTORC1 and mTORC2 activity, respectively, led to cone function decline and structural abnormalities of cone outer segments.[39] Conversely, upregulation of mTORC1 signaling in cones by crossing an RP mouse model with rod-specific *Pten* cKO or *Tsc1* cKO mice, prevents rod or cone degeneration, respectively.[31,91] Similarly, using insulin to stimulate mTOR signaling delays cone loss in an RP model.[30] These findings from mouse models are consistent with clinical trial results using the mTOR inhibitor sirolimus in patients with AMD, which either had no effect or worsened vision.[92,93]

Despite the apparent neuroprotective role for mTORC1 in maintaining photoreceptor health, the long-term effects of elevated mTOR signaling are not always beneficial. For instance, if mTORC1 signaling is elevated in mouse cones, atrophy is observed in the RPE, and lipoproteins that resemble drusen are deposited, as seen in late-stage AMD.[36] Likewise, a chemical model of RP was shown to have increased mTORC1 levels in photoreceptors.[37] In contrast to our findings, degeneration could be slowed down in this model with rapamycin.[37] Another approach to block mTORC1 signaling involves the use of metformin, which activates AMPK signaling, an inhibitor of mTOR.[94] Strikingly, metformin treatment has neuroprotective effects in genetic and chemical models of retinal degeneration,[95] indicating mTOR-independent molecular events also contribute in this setting.

One possibility is that mTORC1 signaling impacts photoreceptor health by altering metabolism, an attractive possibility given that photoreceptors are among the most metabolically active cells in the body. Indeed, when mTOR activity is elevated in photoreceptors, several metabolic genes are upregulated, including the glucose transport gene, *Glut1*, and glycolysis-pathway genes, *Hk2*, *Pkm2*, and *G6pd*.[31] Glucose 6-phosphate dehydrogenase (G6PD) is part of the pentose phosphate pathway (PPP), an offshoot of glycolysis that maintains redox balance by producing nicotinamide adenine dinucleotide phosphate (NADPH), a strong reducing agent.[96] G6PD/NADPH promote cell survival by triggering the phosphorylation and inactivation of caspase 2 ($CASP_2$), preventing $CASP_2$-dependent cell death.[97] Because a $CASP_2$ KO improves cone survival in a mouse model of RP, and $CASP_2$ is NADPH-regulated, by extension, glucose metabolism and NADPH production are essential for cone survival in this RP model.[31] The pro-survival effect of elevated glycolysis and lactate production is similarly observed in rods in a $Rho^{P23H/+}$ model of RP, as demonstrated using genetic methods to disinhibit ENO1, a glycolytic enzyme.[98] Thus, in the context of degenerative photoreceptor disease, activating glycolysis has pro-survival effects.

Even though elevated glycolysis supports photoreceptor survival in the models of neurodegeneration discussed above, we found that 2DG-mediated inhibition of glycolysis, which we confirmed reduces lactate levels, does not prevent photoreceptor degeneration in *Pten* RPC-cKO retinas. A possible explanation is that when glucose uptake is reduced in the retina, anaplerotic substrates, such as lactate, amino acids, and fatty acids, can instead be used for energy production.[13] Thus, in the *Pten* RPC-cKO retina, the effect of 2DG may be minor due to a reliance on anaplerotic metabolism. Indeed, by reducing retinal glucose, which is mainly taken up by the RPE through GLUT1, anaplerotic metabolism is triggered in retinal explants.[13] Another explanation may be that rod photoreceptors do not solely rely on glycolysis for energy production, but can also use, and may even prefer, oxidative phosphorylation, which is essential for photoreceptor survival.[13] Although earlier findings suggested that

Investigative Ophthalmology & Visual Science

rods depend solely on aerobic glycolysis, these studies may have been influenced by a disruption of the RPE in the analyzed tissue.[14] Indeed, removing the RPE disrupts metabolic homeostasis, increasing glycolytic activity in retinal explants.[13] Finally, because *Pten* loss increases mitochondrial respiration and elevates oxidative stress,[99] increased oxidative metabolism in *Pten*-deleted photoreceptors could trigger increased free fatty acids (FFAs) production.[100] Subsequently, FFAs can directly induce oxidative stress by overloading mitochondria with fuel, leading to elevated reactive oxygen species production, which can induce cellular damage and degeneration.

In summary, we analyzed the role of *Pten* in photoreceptor survival, both in a congenital model, in which *Pten* was deleted in all retinal cells, or in a rod-specific deletion. We found that deleting *Pten* in all retinal cell types or only in rod photoreceptors triggers photoreceptor degeneration, albeit with a more severe phenotype observed in the RPC-specific cKO. Intriguingly, rapamycin exacerbated the photoreceptor degeneration phenotype, indicating that suppressing mTORC1 signaling in the context of a *Pten* cKO further exacerbates whatever pro-degenerative signals are present. These data suggest that in the context of a *Pten* cKO, mTORC1 signaling is protective. Deletion of *Pten* in all retinal cell types results in characteristics similar to AMD with evidence of angiogenesis and deposit formation positive for amyloid-β antibodies on immunostaining. Taken together, these mice may serve as a good model of AMD for future therapeutic development.

Acknowledgments

The authors thank Petia Stefanova in the SRI Histology Facility for assistance with sectioning, and Zeinab Noroozian in the Aubert lab for immunostaining assistance.

Supported by the Canadian Institutes of Health Research (CIHR) PJT 180243 to CS and YT, and PJT – 400973 to IA and CS. JH was supported by a Canada Graduate Scholarship – Doctoral (CGS-D)/CIHR award, Vision Science Research Program Scholarship, Ontario Graduate Scholarship and R.O. Torrance Bursary. CS holds the Dixon Family Chair in Ophthalmology Research at the Sunnybrook Research Institute.

Disclosure: **J. Hanna**, None; **Y. Touahri**, None; **A. Pak**, None; **L.A. David**, None; **E. van Oosten**, None; **R. Dixit**, None; **L.M. Vecchio**, None; **D.N. Mehta**, None; **R. Minamisono**, None; **I. Aubert**, None; **C. Schuurmans**, None

References

1. Jeon CJ, Strettoi E, Masland RH. The major cell populations of the mouse retina. *J Neurosci*. 1998;18:8936–8946.
2. Masland RH. The fundamental plan of the retina. *Nat Neurosci*. 2001;4:877–886.
3. Baden T, Euler T, Berens P. Understanding the retinal basis of vision across species. *Nat Rev Neurosci*. 2020;21:5–20.
4. Swaroop A, Kim D, Forrest D. Transcriptional regulation of photoreceptor development and homeostasis in the mammalian retina. *Nat Rev Neurosci*. 2010;11:563–576.
5. Manley A, Meshkat BI, Jablonski MM, Hollingsworth TJ. Cellular and molecular mechanisms of pathogenesis underlying inherited retinal dystrophies. *Biomolecules*. 2023;13:271.
6. Guillonneau X, Eandi CM, Paques M, Sahel JA, Sapieha P, Sennlaub F. On phagocytes and macular degeneration. *Prog Retin Eye Res*. 2017;61:98–128.
7. Sanie-Jahromi F, Nowroozzadeh MH. RPE based gene and cell therapy for inherited retinal diseases: a review. *Exp Eye Res*. 2022;217:108961.
8. Biel M, Seeliger M, Pfeifer A, et al. Selective loss of cone function in mice lacking the cyclic nucleotide-gated channel CNG3. *Proc Natl Acad Sci USA*. 1999;96:7553–7557.
9. Yang RB, Robinson SW, Xiong WH, Yau KW, Birch DG, Garbers DL. Disruption of a retinal guanylyl cyclase gene leads to cone-specific dystrophy and paradoxical rod behavior. *J Neurosci*. 1999;19:5889–5897.
10. Cho KI, Haque M, Wang J, et al. Distinct and atypical intrinsic and extrinsic cell death pathways between photoreceptor cell types upon specific ablation of Ranbp2 in cone photoreceptors. *PLoS Genet*. 2013;9:e1003555.
11. Xu J, Morris LM, Michalakis S, et al. CNGA3 deficiency affects cone synaptic terminal structure and function and leads to secondary rod dysfunction and degeneration. *Invest Ophthalmol Vis Sci*. 2012;53:1117–1129.
12. Wong WL, Su X, Li X, et al. Global prevalence of age-related macular degeneration and disease burden projection for 2020 and 2040: a systematic review and meta-analysis. *Lancet Glob Health*. 2014;2:e106–e116.
13. Chen Y, Zizmare L, Calbiague V, et al. Retinal metabolism displays evidence for uncoupling of glycolysis and oxidative phosphorylation via Cori-, Cahill-, and mini-Krebs-cycle. *eLife*. 2024;12:RP91141.
14. Kanow MA, Giarmarco MM, Jankowski CS Sr, et al. Biochemical adaptations of the retina and retinal pigment epithelium support a metabolic ecosystem in the vertebrate eye. *Elife*. 2017;6:e28899.
15. Rajala A, Rajala RVS. Age-related changes in the glycolytic enzymes of M2-isoform of pyruvate kinase and fructose-1,6-bisphosphate aldolase: implications to age-related macular degeneration. *Aging Dis*. 2024;15:2271–2283.
16. Nolan ND, Caruso SM, Cui X, Tsang SH. Renormalization of metabolic coupling treats age-related degenerative disorders: an oxidative RPE niche fuels the more glycolytic photoreceptors. *Eye (Lond)*. 2022;36:278–283.
17. Hurley JB. Retina metabolism and metabolism in the pigmented epithelium: a busy intersection. *Annu Rev Vis Sci*. 2021;7:665–692.
18. Chinchore Y, Begaj T, Wu D, Drokhlyansky E, Cepko CL. Glycolytic reliance promotes anabolism in photoreceptors. *Elife*. 2017;6:e25946.
19. Szwed A, Kim E, Jacinto E. Regulation and metabolic functions of mTORC1 and mTORC2. *Physiol Rev*. 2021;101:1371–1426.
20. Mohand-Said S, Hicks D, Simonutti M, et al. Photoreceptor transplants increase host cone survival in the retinal degeneration (rd) mouse. *Ophthalmic Res*. 1997;29:290–297.
21. Mohand-Said S, Deudon-Combe A, Hicks D, et al. Normal retina releases a diffusible factor stimulating cone survival in the retinal degeneration mouse. *Proc Natl Acad Sci USA*. 1998;95:8357–8362.
22. Mohand-Said S, Hicks D, Dreyfus H, Sahel JA. Selective transplantation of rods delays cone loss in a retinitis pigmentosa model. *Arch Ophthalmol*. 2000;118:807–811.
23. Léveillard T, Mohand-Saïd S, Lorentz O, et al. Identification and characterization of rod-derived cone viability factor. *Nat Genet*. 2004;36:755–759.
24. Streichert LC, Birnbach CD, Reh TA. A diffusible factor from normal retinal cells promotes rod photoreceptor survival in an in vitro model of retinitis pigmentosa. *J Neurobiol*. 1999;39:475–490.
25. Gupta N, Brown KE, Milam AH. Activated microglia in human retinitis pigmentosa, late-onset retinal degenera-

Investigative Ophthalmology & Visual Science

tion, and age-related macular degeneration. *Exp Eye Res*. 2003;76:463–471.
26. Komeima K, Rogers BS, Lu L, Campochiaro PA. Antioxidants reduce cone cell death in a model of retinitis pigmentosa. *Proc Natl Acad Sci USA*. 2006;103:11300–11305.
27. Komeima K, Rogers BS, Campochiaro PA. Antioxidants slow photoreceptor cell death in mouse models of retinitis pigmentosa. *J Cell Physiol*. 2007;213:809–815.
28. Lu L, Oveson BC, Jo YJ, et al. Increased expression of glutathione peroxidase 4 strongly protects retina from oxidative damage. *Antioxid Redox Signal*. 2009;11:715–724.
29. Usui S, Komeima K, Lee SY, et al. Increased expression of catalase and superoxide dismutase 2 reduces cone cell death in retinitis pigmentosa. *Mol Ther*. 2009;17:778–786.
30. Punzo C, Kornacker K, Cepko CL. Stimulation of the insulin/mTOR pathway delays cone death in a mouse model of retinitis pigmentosa. *Nat Neurosci*. 2009;12:44–52.
31. Venkatesh A, Ma S, Le YZ, Hall MN, Ruegg MA, Punzo C. Activated mTORC1 promotes long-term cone survival in retinitis pigmentosa mice. *J Clin Invest*. 2015;125:1446–1458.
32. Lin B, Xiong G, Yang W. Ribosomal protein S6 kinase 1 promotes the survival of photoreceptors in retinitis pigmentosa. *Cell Death Dis*. 2018;9:1141.
33. Zhang L, Justus S, Xu Y, et al. Reprogramming towards anabolism impedes degeneration in a preclinical model of retinitis pigmentosa. *Hum Mol Genet*. 2016;25:4244–4255.
34. Zhang L, Du J, Justus S, et al. Reprogramming metabolism by targeting sirtuin 6 attenuates retinal degeneration. *J Clin Invest*. 2016;126:4659–4673.
35. Petit L, Ma S, Cipi J, et al. Aerobic glycolysis is essential for normal rod function and controls secondary cone death in retinitis pigmentosa. *Cell Rep*. 2018;23:2629–2642.
36. Cheng SY, Cipi J, Ma S, et al. Altered photoreceptor metabolism in mouse causes late stage age-related macular degeneration-like pathologies. *Proc Natl Acad Sci USA*. 2020;117:13094–13104.
37. Zhao M, Lv H, Yang N, Peng GH. Rapamycin improved retinal function and morphology in a mouse model of retinal degeneration. *Front Neurosci*. 2022;16:846584.
38. Okamoto T, Ozawa Y, Kamoshita M, et al. The neuroprotective effect of rapamycin as a modulator of the mTOR-NF-kappaB axis during retinal inflammation. *PLoS One*. 2016;11:e0146517.
39. Ma S, Venkatesh A, Langellotto F, et al. Loss of mTOR signaling affects cone function, cone structure and expression of cone specific proteins without affecting cone survival. *Exp Eye Res*. 2015;135:1–13.
40. Comer FI, Parent CA. Phosphoinositides specify polarity during epithelial organ development. *Cell*. 2007;128:239–240.
41. Stambolic V, Suzuki A, de la Pompa JL, et al. Negative regulation of PKB/Akt-dependent cell survival by the tumor suppressor PTEN. *Cell*. 1998;95:29–39.
42. Qian X, Li X, Shi Z, et al. PTEN suppresses glycolysis by dephosphorylating and inhibiting autophosphorylated PGK1. *Mol Cell*. 2019;76:516–527.e517.
43. Hanna J, Touahri Y, Pak A, et al. Glycolytic flux controls retinal progenitor cell differentiation via regulating WNT signaling. *eLife*. 2024;13:RP100604.
44. Ohtake Y, Hayat U, Li S. PTEN inhibition and axon regeneration and neural repair. *Neural Regen Res*. 2015;10:1363–1368.
45. Park KK, Liu K, Hu Y, et al. Promoting axon regeneration in the adult CNS by modulation of the PTEN/mTOR pathway. *Science*. 2008;322:963–966.
46. Skelton PD, Stan RV, Luikart BW. The role of PTEN in neurodevelopment. *Mol Neuropsychiatry*. 2020;5:60–71.
47. Tachibana N, Cantrup R, Dixit R, et al. Pten regulates retinal amacrine cell number by modulating Akt, Tgfbeta, and Erk signaling. *J Neurosci*. 2016;36:9454–9471.
48. Tachibana N, Touahri Y, Dixit R, et al. Hamartoma-like lesions in the mouse retina: an animal model of Pten hamartoma tumour syndrome. *Dis Model Mech*. 2018;11:dmm031005.
49. Touahri Y, Hanna J, Tachibana N, et al. Pten regulates endocytic trafficking of cell adhesion and Wnt signaling molecules to pattern the retina. *Cell Rep*. 2024;43:114005.
50. Cantrup R, Dixit R, Palmesino E, et al. Cell-type specific roles for PTEN in establishing a functional retinal architecture. *PLoS One*. 2012;7:e32795.
51. Jo HS, Kang KH, CO Joe, Kim JW. Pten coordinates retinal neurogenesis by regulating Notch signalling. *EMBO J*. 2012;31:817–828.
52. Sakagami K, Chen B, Nusinowitz S, Wu H, Yang XJ. PTEN regulates retinal interneuron morphogenesis and synaptic layer formation. *Mol Cell Neurosci*. 2012;49:171–183.
53. Backman SA, Stambolic V, Suzuki A, et al. Deletion of Pten in mouse brain causes seizures, ataxia and defects in soma size resembling Lhermitte-Duclos disease. *Nat Genet*. 2001;29:396–403.
54. Marquardt T, Ashery-Padan R, Andrejewski N, Scardigli R, Guillemot F, Gruss P. Pax6 is required for the multipotent state of retinal progenitor cells. *Cell*. 2001;105:43–55.
55. Le YZ, Zheng L, Zheng W, et al. Mouse opsin promoter-directed Cre recombinase expression in transgenic mice. *Mol Vis*. 2006;12:389–398.
56. Brennenstuhl C, Tanimoto N, Burkard M, et al. Targeted ablation of the Pde6h gene in mice reveals cross-species differences in cone and rod phototransduction protein isoform inventory. *J Biol Chem*. 2015;290:10242–10255.
57. Kohl S, Baumann B, Rosenberg T, et al. Mutations in the cone photoreceptor G-protein alpha-subunit gene GNAT2 in patients with achromatopsia. *Am J Hum Genet*. 2002;71:422–425.
58. Makino CL, Dodd RL, Chen J, et al. Recoverin regulates light-dependent phosphodiesterase activity in retinal rods. *J Gen Physiol*. 2004;123:729–741.
59. van Huet RA, Collin RW, Siemiatkowska AM, et al. IMPG2-associated retinitis pigmentosa displays relatively early macular involvement. *Invest Ophthalmol Vis Sci*. 2014;55:3939–3953.
60. Schor NF, Bianchi DW. Neurodevelopmental clues to neurodegeneration. *Pediatr Neurol*. 2021;123:67–76.
61. Cook HL, Patel PJ, Tufail A. Age-related macular degeneration: diagnosis and management. *Br Med Bull*. 2008;85:127–149.
62. Keeling E, Lotery AJ, Tumbarello DA, Ratnayaka JA. Impaired cargo clearance in the retinal pigment epithelium (RPE) underlies irreversible blinding diseases. *Cells*. 2018;7:16.
63. Kim JW, Kang KH, Burrola P, Mak TW, Lemke G. Retinal degeneration triggered by inactivation of PTEN in the retinal pigment epithelium. *Genes Dev*. 2008;22:3147–3157.
64. Mei X, Chaffiol A, Kole C, et al. The thioredoxin encoded by the rod-derived cone viability factor gene protects cone photoreceptors against oxidative stress. *Antioxid Redox Signal*. 2016;24:909–923.
65. Bringmann A, Iandiev I, Pannicke T, et al. Cellular signaling and factors involved in Muller cell gliosis: neuroprotective and detrimental effects. *Prog Retin Eye Res*. 2009;28:423–451.

Investigative Ophthalmology & Visual Science

66. Díaz-Lezama N, Kajtna J, Wu J, Ayten M, Koch SF. Microglial and macroglial dynamics in a model of retinitis pigmentosa. *Vision Res*. 2023;210:108268.
67. Wu KH, Madigan MC, Billson FA, Penfold PL. Differential expression of GFAP in early v late AMD: a quantitative analysis. *Br J Ophthalmol*. 2003;87:1159–1166.
68. de Hoz R, Rojas B, Ramirez AI, et al. Retinal macroglial responses in health and disease. *Biomed Res Int*. 2016;2016:2954721.
69. Ko IG. Therapeutic strategies against apoptosis and gliosis. *Int Neurourol J*. 2020;24:65–66.
70. Bringmann A, Wiedemann P. Muller glial cells in retinal disease. *Ophthalmologica*. 2012;227:1–19.
71. Bressler SB. Introduction: Understanding the role of angiogenesis and antiangiogenic agents in age-related macular degeneration. *Ophthalmology*. 2009;116(10 Suppl):S1–S7.
72. Hanna J, Yucel YH, Zhou X, Mathieu E, Paczka-Giorgi LA, Gupta N. Progressive loss of retinal blood vessels in a live model of retinitis pigmentosa. *Can J Ophthalmol*. 2018;53:391–401.
73. Milam AH, Li ZY, Fariss RN. Histopathology of the human retina in retinitis pigmentosa. *Prog Retin Eye Res*. 1998;17:175–205.
74. Tian T, Nan KJ, Wang SH, et al. PTEN regulates angiogenesis and VEGF expression through phosphatase-dependent and -independent mechanisms in HepG2 cells. *Carcinogenesis*. 2010;31:1211–1219.
75. Miller JW. Age-related macular degeneration revisited–piecing the puzzle: the LXIX Edward Jackson memorial lecture. *Am J Ophthalmol*. 2013;155:1–35.e13.
76. Khan KN, Mahroo OA, Khan RS, et al. Differentiating drusen: Drusen and drusen-like appearances associated with ageing, age-related macular degeneration, inherited eye disease and other pathological processes. *Prog Retin Eye Res*. 2016;53:70–106.
77. Mullins RF, Russell SR, Anderson DH, Hageman GS. Drusen associated with aging and age-related macular degeneration contain proteins common to extracellular deposits associated with atherosclerosis, elastosis, amyloidosis, and dense deposit disease. *FASEB J*. 2000;14:835–846.
78. He L, Hou X, Kanel G, et al. The critical role of AKT2 in hepatic steatosis induced by PTEN loss. *Am J Pathol*. 2010;176:2302–2308.
79. Rudajev V, Novotny J. Cholesterol as a key player in amyloid β-mediated toxicity in Alzheimer's disease. *Front Mol Neurosci*. 2022;15:937056.
80. Clement CG, Truong LD. An evaluation of Congo red fluorescence for the diagnosis of amyloidosis. *Hum Pathol*. 2014;45:1766–1772.
81. Fernandes SA, Demetriades C. The multifaceted role of nutrient sensing and mTORC1 signaling in physiology and aging. *Front Aging*. 2021;2:707372.
82. Fabre M, Mateo L, Lamaa D, et al. Recent advances in age-related macular degeneration therapies. *Molecules*. 2022;27:5089.
83. Wu KY, Kulbay M, Toameh D, Xu AQ, Kalevar A, Tran SD. Retinitis pigmentosa: novel therapeutic targets and drug development. *Pharmaceutics*. 2023;15:685.
84. Dentchev T, Milam AH, Lee VM, Trojanowski JQ, Dunaief JL. Amyloid-beta is found in drusen from some age-related macular degeneration retinas, but not in drusen from normal retinas. *Mol Vis*. 2003;9:184–190.
85. Ratnayaka JA, Serpell LC, Lotery AJ. Dementia of the eye: the role of amyloid beta in retinal degeneration. *Eye (Lond)*. 2015;29:1013–1026.
86. Cahill MT, Mruthyunjaya P, Bowes Rickman C, Toth CA. Recurrence of retinal pigment epithelial changes after macular translocation with 360 degrees peripheral retinectomy for geographic atrophy. *Arch Ophthalmol*. 2005;123:935–938.
87. Khurana RN, Fujii GY, Walsh AC, Humayun MS, de Juan E, Jr., Sadda SR. Rapid recurrence of geographic atrophy after full macular translocation for nonexudative age-related macular degeneration. *Ophthalmology*. 2005;112:1586–1591.
88. Curcio CA. Antecedents of soft drusen, the specific deposits of age-related macular degeneration, in the biology of human macula. *Invest Ophthalmol Vis Sci*. 2018;59:AMD182–AMD194.
89. Curcio CA. Soft drusen in age-related macular degeneration: biology and targeting via the oil spill strategies. *Invest Ophthalmol Vis Sci*. 2018;59:AMD160–AMD181.
90. Abdelfattah NS, Zhang H, Boyer DS, et al. Drusen volume as a predictor of disease progression in patients with late age-related macular degeneration in the fellow eye. *Invest Ophthalmol Vis Sci*. 2016;57:1839–1846.
91. Zhang L, Justus S, Xu Y, et al. Reprogramming towards anabolism impedes degeneration in a preclinical model of retinitis pigmentosa. *Hum Mol Genet*. 2016;25:4244–4255.
92. Petrou PA, Cunningham D, Shimel K, et al. Intravitreal sirolimus for the treatment of geographic atrophy: results of a phase I/II clinical trial. *Invest Ophthalmol Vis Sci*. 2014;56:330–338.
93. Wong WT, Dresner S, Forooghian F, et al. Treatment of geographic atrophy with subconjunctival sirolimus: results of a phase I/II clinical trial. *Invest Ophthalmol Vis Sci*. 2013;54:2941–2950.
94. Amin S, Lux A, O'Callaghan F. The journey of metformin from glycaemic control to mTOR inhibition and the suppression of tumour growth. *Br J Clin Pharmacol*. 2019;85:37–46.
95. Xu L, Kong L, Wang J, Ash JD. Stimulation of AMPK prevents degeneration of photoreceptors and the retinal pigment epithelium. *Proc Natl Acad Sci USA*. 2018;115:10475–10480.
96. Düvel K, Yecies JL, Menon S, et al. Activation of a metabolic gene regulatory network downstream of mTOR complex 1. *Mol Cell*. 2010;39:171–183.
97. Nutt LK, Margolis SS, Jensen M, et al. Metabolic regulation of oocyte cell death through the CaMKII-mediated phosphorylation of caspase-2. *Cell*. 2005;123:89–103.
98. Nelson TS, Simpson C, Dyka FM, Dinculescu A, Smith WC. A modified arrestin1 increases lactate production in the retina and slows retinal degeneration. *Hum Gene Ther*. 2022;33:695–707.
99. Li Y, He L, Zeng N, et al. Phosphatase and tensin homolog deleted on chromosome 10 (PTEN) signaling regulates mitochondrial biogenesis and respiration via estrogen-related receptor α (ERRα). *J Biol Chem*. 2013;288:25007–25024.
100. Pan WW, Wubben TJ, Besirli CG. Photoreceptor metabolic reprogramming: current understanding and therapeutic implications. *Commun Biol*. 2021;4:245.

Investigative Ophthalmology & Visual Science